

RF Basics I and II

Frank Gerigk

CERN, Geneva, Switzerland

Abstract

Maxwell's equations are introduced in their general form, together with a basic set of mathematical operations needed to work with them. After simplifying and adapting the equations for application to radio frequency problems, we derive the most important formulae and characteristic quantities for cavities and waveguides. Several practical examples are given to demonstrate the use of the derived equations and to explain the importance of the most common figures of merit.

1 Introduction to Maxwell's equations

1.1 Maxwell's equations

Maxwell's equations were published in their earliest form in 1861–1862 in a paper entitled “On physical lines of force” by the Scottish physicist and mathematician James Clerk Maxwell. They represent a uniquely complete set of equations that covers all areas of electrostatic and magnetostatic problems, as well as electrodynamic problems, of which radio frequency (RF) engineering is only a subset. Surprisingly, they include the effects of relativity even though they were conceived much earlier than Einstein's theories.

In differential form, Maxwell's equations can be written as

$$\nabla \times \mathbf{H} = \mathbf{J} + \frac{\partial \mathbf{D}}{\partial t}, \quad (1)$$

$$\nabla \times \mathbf{E} = -\frac{\partial \mathbf{B}}{\partial t}, \quad \text{Maxwell's equations} \quad (2)$$

$$\nabla \cdot \mathbf{D} = q_v, \quad (3)$$

$$\nabla \cdot \mathbf{B} = 0, \quad (4)$$

where the field components and constants are defined as follows:

$$\begin{array}{ll} \mathbf{E}, & \text{electric field (V/m)} \\ \mathbf{D} = \epsilon_0 \epsilon_r \mathbf{E}, & \text{dielectric displacement (A s/m}^2\text{)} \end{array} \quad (5)$$

$$\begin{array}{ll} \mathbf{B}, & \text{magnetic induction, magnetic flux density (T)} \end{array}$$

$$\begin{array}{ll} \mathbf{H} = \frac{1}{\mu_0 \mu_r} \mathbf{B}, & \text{magnetic field strength or field intensity (A/m)} \end{array} \quad (6)$$

$$\begin{array}{ll} \mathbf{J} = \kappa \mathbf{E}, & \text{electric current density (A/m}^2\text{)} \end{array} \quad (7)$$

$$\begin{array}{ll} \frac{d}{dt} \mathbf{D}, & \text{displacement current (A/m}^2\text{)} \\ \epsilon_0 = 8.854 \cdot 10^{-12}, & \text{electric field constant (F/m)} \end{array} \quad (8)$$

$$\begin{array}{ll} \epsilon_r, & \text{relative dielectric constant} \end{array}$$

$$\begin{array}{ll} \mu_0 = 4\pi \cdot 10^{-7}, & \text{magnetic field constant (H/m)} \end{array} \quad (9)$$

$$\begin{array}{ll} \mu_r, & \text{relative permeability constant} \end{array}$$

$$\begin{array}{ll} \kappa. & \text{electrical conductivity (S/m)} \end{array}$$

In the following sections, we shall see that most of the important RF formulae can be derived in a few lines from Maxwell's equations.

1.2 Basic vector analysis and its application to Maxwell's equations

In order to make efficient use of Maxwell's equations, some basic vector analysis is needed, which is introduced in this section. More detailed introductions can be found in a number of textbooks, such as for instance the excellent *Feynman Lectures on Physics* [1].

Gradient of a potential

The gradient of a potential ϕ is the derivative of the potential function $\phi(x,y,z)$ in all directions of a particular coordinate system (e.g., x, y, z). The result is a vector that tells us how much the potential changes in different directions. Applied to the geographical profile of a mountain landscape, the gradient describes the slope of the landscape in all directions. The mathematical sign that is used for the gradient of a potential is the 'nabla operator'; applied to a Cartesian coordinate system, one can write

$$\nabla\Phi = \begin{pmatrix} \frac{\partial}{\partial x} \\ \frac{\partial}{\partial y} \\ \frac{\partial}{\partial z} \end{pmatrix} \Phi = \begin{pmatrix} \frac{\partial\Phi}{\partial x} \\ \frac{\partial\Phi}{\partial y} \\ \frac{\partial\Phi}{\partial z} \end{pmatrix}. \quad \text{gradient of a potential} \quad (10)$$

The expressions for the gradient in cylindrical and spherical coordinate systems are given in Appendices B and C.

Divergence of a vector field

The divergence of a vector field \mathbf{a} tells us if the vector field has a source. If the resulting scalar expression is zero, we have a 'source-free' vector field, as in the case of the magnetic field. From basic physics, we know that there are no magnetic monopoles, which is why magnetic field lines are always closed. In Maxwell's equations (4), this property is included by means of the fact that the divergence of the magnetic induction \mathbf{B} equals zero.

In Cartesian coordinates, the divergence of a vector field is defined as

$$\nabla \cdot \mathbf{a} = \begin{pmatrix} \frac{\partial}{\partial x} \\ \frac{\partial}{\partial y} \\ \frac{\partial}{\partial z} \end{pmatrix} \cdot \begin{pmatrix} a_x \\ a_y \\ a_z \end{pmatrix} = \frac{\partial a_x}{\partial x} + \frac{\partial a_y}{\partial y} + \frac{\partial a_z}{\partial z}. \quad \text{divergence of a vector} \quad (11)$$

The expressions for cylindrical and spherical coordinate systems are given in Appendices B and C.

Curl of a vector field

When we form the curl of a vector, we are interested in knowing if there are any curls or eddies in the field. Let us imagine that we are looking at the flow of water in a cooling pipe. To check for curls, we can use a stick around which a ball can rotate freely. We position a Cartesian coordinate system at an arbitrary origin and align the stick first with the x axis, and then with the y and z axes. If the ball starts rotating in any of these positions, then we know that the curl of the vector field describing the water flow is non-zero in the direction of the respective axis. The curl of a vector \mathbf{a} is therefore also a vector, because its information is direction-specific. Its mathematical form in Cartesian coordinates is defined as

$$\begin{aligned}\nabla \times \mathbf{a} &= \begin{pmatrix} \frac{\partial}{\partial x} \\ \frac{\partial}{\partial y} \\ \frac{\partial}{\partial z} \end{pmatrix} \times \begin{pmatrix} a_x \\ a_y \\ a_z \end{pmatrix} \\ &= \det \begin{pmatrix} \mathbf{u}_x & \mathbf{u}_y & \mathbf{u}_z \\ \frac{\partial}{\partial x} & \frac{\partial}{\partial y} & \frac{\partial}{\partial z} \\ a_x & a_y & a_z \end{pmatrix} = \begin{pmatrix} \frac{\partial a_z}{\partial y} - \frac{\partial a_y}{\partial z} \\ \frac{\partial a_x}{\partial z} - \frac{\partial a_z}{\partial x} \\ \frac{\partial a_y}{\partial x} - \frac{\partial a_x}{\partial y} \end{pmatrix}.\end{aligned}\quad \text{curl of a vector} \quad (12)$$

The *unit* vectors \mathbf{u}_n have no physical meaning and simply point in the x , y , and z directions. They have a constant length of 1. The expressions for cylindrical and spherical coordinate systems can be found in Appendices B and C.

Second derivatives

In some instances, we have to make use of second derivatives. One of the expressions that is used regularly in electrodynamics is the Laplace operator $\Delta = \nabla^2$, which—since the operator itself is scalar—can be applied to both scalar fields and vector fields:

$$\Delta\phi = \nabla \cdot (\nabla\phi) = \nabla^2\phi = \frac{\partial^2\phi}{\partial x^2} + \frac{\partial^2\phi}{\partial y^2} + \frac{\partial^2\phi}{\partial z^2}.\quad \text{Laplace operator} \quad (13)$$

The expressions for cylindrical and spherical coordinate systems can be found in Appendices B and C.

We also introduce two interesting identities:

$$\nabla \times (\nabla\phi) = 0, \quad (14)$$

$$\nabla \cdot (\nabla \times \mathbf{a}) = 0. \quad (15)$$

Equation (14) tells us that if the curl of a vector equals zero, then this vector can be written as the gradient of a potential. This feature can save us a lot of writing when we are dealing with complicated three-dimensional expressions for electric and magnetic fields, and we shall use this principle later on to define non-physical potential functions that can describe (via derivatives) complete three-dimensional vector functions.

In the same way, Eq. (15) can (and will) be used to describe divergence-free fields with simple ‘vector potentials’.

1.3 Useful theorems by Gauss and Stokes

The theorems of Gauss and Stokes are some of the most commonly used transformations in this chapter, and therefore we shall take a moment to explain the concepts of them.

Gauss’s theorem

Gauss’s theorem not only saves us a lot of mathematics but also has a very useful physical interpretation when applied to Maxwell’s equations. Mathematically speaking, we transform a volume integral over the divergence of a vector into a surface integral over the vector itself:

$$\int_V \underbrace{\nabla \cdot \mathbf{a}}_{\text{‘sources’}} dV = \oint_S \mathbf{a} \cdot d\mathbf{S}.\quad \text{Gauss’s theorem} \quad (16)$$

The surface on the right-hand side of the theorem is the one that surrounds the volume on the left-hand side. If we remember that the divergence of a vector field is equal to its sources, Gauss's theorem tells us that:

- The vector flux through a closed surface equals the sources of flux within the enclosed volume.
- If there are no sources, the amounts of flux entering and leaving the volume must be equal.

These statements can be applied directly to Maxwell's equations. Using Eq. (3) and applying Gauss's theorem, we obtain

$$\int_V \nabla \cdot \mathbf{E} dV = \oint_S \mathbf{E} \cdot d\mathbf{S} = \frac{Q}{\epsilon} \quad (17)$$

(Fig. 1), which means that one can calculate the amount of charge in a volume simply by integrating the electric flux lines over any closed surface that surrounds the charge, or vice versa.

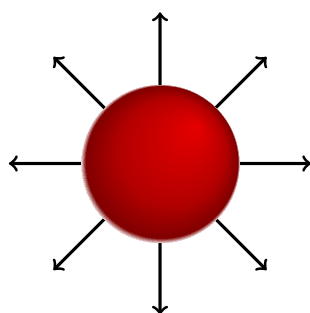


Fig. 1: Example of electric flux lines emanating from electric charge in the centre of a sphere

The same trick can be applied to the source-free magnetic field. Here, we use Eq. (4) and obtain

$$\int_V \nabla \cdot \mathbf{B} dV = \oint_S \mathbf{B} \cdot d\mathbf{S} = 0. \quad (18)$$

Equation (18) gives us the proof of what was already stated earlier: magnetic field lines have no sources ($\nabla \cdot \mathbf{B} = 0$), and therefore the magnetic flux lines are always closed and have neither sources nor sinks. If magnetic flux lines enter a volume, then they also have to leave that volume (Fig. 2).

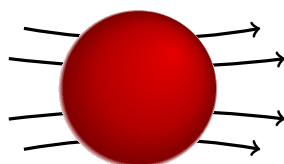


Fig. 2: Example of magnetic flux lines penetrating a sphere

Stokes's theorem

Whereas Gauss's theorem is useful for equations involving the divergence of a vector, Stokes's theorem offers a similar simplification for equations that contain the curl of a vector. With Stokes's theorem, we can transform surface integrals over the curl of a vector into closed line integrals over the vector itself:

$$\int_A (\nabla \times \mathbf{a}) \cdot d\mathbf{A} = \oint_C \mathbf{a} \cdot d\mathbf{l}. \quad \text{Stokes's theorem} \quad (19)$$

One can interpret Stokes's theorem with the help of Fig. 3 as follows:

- the area integral over the curl of a vector field can be calculated from a line integral along its closed borders, or
- the field lines of a vector field with non-zero curl must be closed contours.

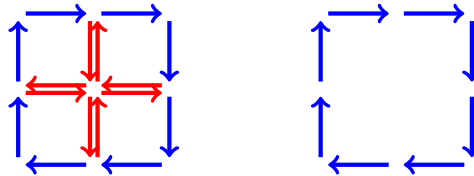


Fig. 3: Illustration of Stokes's theorem

The meaning of these statements becomes immediately clear when we apply Stokes's theorem to Maxwell's equation (1):

$$\int_A (\nabla \times \mathbf{H}) \cdot d\mathbf{A} = \oint_C \mathbf{H} \cdot d\mathbf{l} = \int_A \left(\mathbf{J} + \frac{d\mathbf{D}}{dt} \right) \cdot d\mathbf{A}. \quad (20)$$

In the electrostatic case, the time derivative disappears and the area integral over the current density may, for instance, be the current flowing in an electric wire as shown in Fig. 4. This means that with a one-line manipulation of Maxwell's equations, we have derived Ampère's law, which tells us that every current induces a circular magnetic field around itself, whose strength can be calculated from a simple closed line integral along a circular path with the current at its centre.

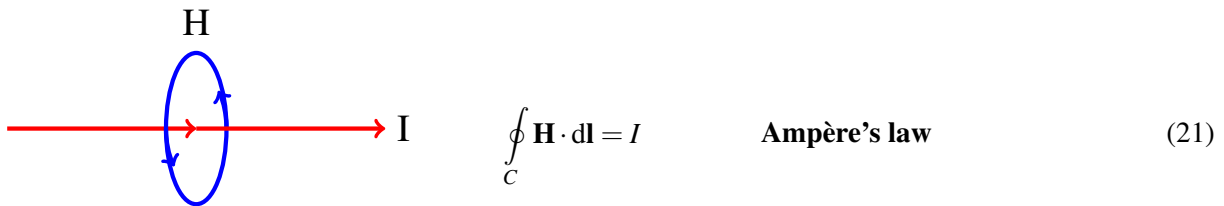


Fig. 4: Illustration of Ampère's law

With similar ease, we can derive Faraday's induction law, which is the basis of every electric motor and generator. All we have to do is apply Stokes's theorem to Maxwell's equation (2):

$$\int_A (\nabla \times \mathbf{E}) \cdot d\mathbf{A} = \underbrace{\oint_C \mathbf{E} \cdot d\mathbf{l}}_{V_i} = - \underbrace{\frac{d}{dt} \int_A \mathbf{B} \cdot d\mathbf{A}}_{\frac{d\psi_m}{dt}}, \quad (22)$$

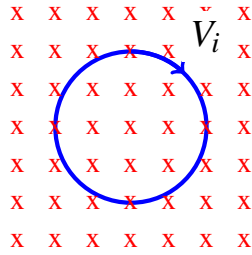
and again, after one line, we obtain one of the fundamental laws of electrical engineering.

Faraday's law tells us that an electric voltage is induced in a loop if the magnetic flux ψ penetrating the loop changes over time, as shown in Fig. 5. Alternatively, one can change the flux by moving the loop in or out of a static magnetic field.

I hope that these examples have convinced you that Maxwell's equations are indeed very powerful, and that with a bit of vector analysis we really can derive everything we need for RF engineering (although maybe not always in one line ...).

1.4 Displacement current

Although most people have an idea of what electric and magnetic fields are, the displacement current $d\mathbf{D}/dt$ is often not so well understood. Since it is vital for the propagation of electromagnetic waves,



$$V_i = -\frac{d\psi_m}{dt} \quad \text{Faraday's induction law} \quad (23)$$

Fig. 5: Illustration of Faraday's induction law

we shall spend a few lines studying this quantity. We start by deriving and interpreting the continuity equation, and then look at a simple practical example.

We apply the divergence to Maxwell's equation (1):

$$\underbrace{\nabla \cdot (\nabla \times \mathbf{H})}_{\equiv 0} = \nabla \cdot \mathbf{J} + \underbrace{\nabla \cdot \frac{d\mathbf{D}}{dt}}_{\frac{d}{dt}\rho_v} \quad (24)$$

Using Maxwell's equation (3), we have made an association between the 'sources of the displacement current' $\nabla \cdot (d\mathbf{D}/dt)$ and the 'rate of change of electric charge' $(d/dt)\rho_v$. Using the identity (15), we obtain the continuity equation

$$\nabla \cdot \mathbf{J} = -\frac{d}{dt}\rho_v, \quad \text{continuity equation} \quad (25)$$

to which we apply a volume integral and Gauss's theorem (16):

$$\int_V \nabla \cdot \mathbf{J} dV = \oint_S \mathbf{J} \cdot d\mathbf{S} = \sum I_n = -\frac{d}{dt} \int_V \rho_v dV. \quad \text{continuity equation} \quad (26)$$

In this form, the interpretation is very straightforward, and we can state that:

- if the amount of electric charge in a volume is changing over time, a current needs to flow; or, more poignantly, electric charges cannot be destroyed.

Now, it is good to know that electric charges cannot be destroyed, but that does not yet help us to understand the displacement current. For this purpose, we go back to Eq. (24) and this time we do not replace the expression for the displacement current. Instead, we apply a volume integral and Gauss's theorem and obtain

$$\oint_S \mathbf{J} \cdot d\mathbf{S} = \sum I_n = -\frac{d}{dt} \oint_S \mathbf{D} d\mathbf{S} = -\frac{d}{dt} \int_V \rho_v dV, \quad (27)$$

which we can apply to the simple geometry of a capacitor shown in Fig. 6, which is charged by a static current I .

If we assume a small volume with a surface S around one of the capacitor plates, then we can directly interpret Eq. (27): the current I , which enters the volume V on the left, equals the flux integral of the displacement current $-(d/dt)\mathbf{D}$, which leaves the volume V on the right. This means that the displacement current can be understood as a 'current without charge transport', which in this case can only exist because of the rate of change of the electric charge $-(d/dt) \int_V \rho_v dV$ on the left capacitor plate.

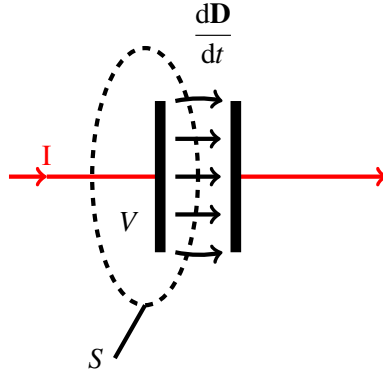


Fig. 6: Example of a displacement current: charging of a capacitor

1.5 Boundary conditions

Before we try to calculate electromagnetic fields in accelerating cavities, we need to understand how these fields behave close to material boundaries, for example the electrically conducting walls of a cavity. Using Stokes's and Gauss's theorems, we can quickly derive these boundary conditions.

Field components parallel to a material boundary

We start with the field components (E_{\parallel} , H_{\parallel}) parallel to a surface between two materials, as depicted in Fig. 7. We define a small surface ΔA , which is perpendicular to the boundary and encloses a small cross-section of the boundary area. Then we integrate Maxwell's equations (1) and (2) over this area and apply Stokes's theorem:

$$\int_A \nabla \times \mathbf{H} \cdot d\mathbf{A} = \oint_C \mathbf{H} \cdot d\mathbf{l} = \underbrace{\int_A \mathbf{J} \cdot d\mathbf{A}}_{=i\Delta l} + \underbrace{\frac{d}{dt} \int_A \mathbf{D} \cdot d\mathbf{A}}_{\rightarrow 0 \text{ for } A \rightarrow 0}, \quad (28)$$

$$\int_A \nabla \times \mathbf{E} \cdot d\mathbf{A} = \oint_C \mathbf{E} \cdot d\mathbf{l} = - \underbrace{\frac{d}{dt} \int_A \mathbf{B} \cdot d\mathbf{A}}_{\rightarrow 0 \text{ for } A \rightarrow 0}. \quad (29)$$

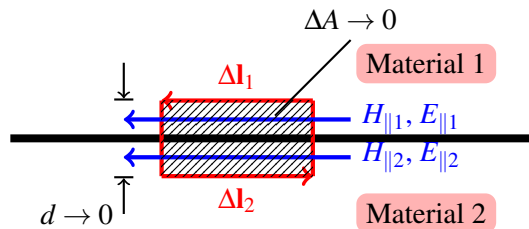


Fig. 7: Boundary conditions parallel to a material boundary

Using Stokes's theorem, the area integrals over A are transformed into line integrals around the contour C of the area. If the width d of the area (see Fig. 7) is now reduced to zero, the calculation of the contour integral simplifies to a multiplication of the field components E_{\parallel} and H_{\parallel} by the path elements Δl . The area integrals over \mathbf{D} and \mathbf{B} vanish and the area integral over the current density \mathbf{J} is replaced by a surface current, which may flow in the boundary plane between the two materials, times the path

element Δl . This results in the following boundary conditions:

$$\begin{aligned} H_{\parallel 1} - H_{\parallel 2} &= i', \\ E_{\parallel 1} &= E_{\parallel 2}. \end{aligned} \quad \begin{array}{l} \text{conditions for magnetic and} \\ \text{electric fields parallel to a} \\ \text{material boundary} \end{array} \quad (30)$$

In the case of a waveguide or an accelerator cavity, we generally assume one of the materials (e.g., material 2) to be an ideal electrical conductor, and in that case the electric and magnetic field components in this material vanish, so that we obtain

$$\begin{aligned} H_{\parallel 1} &= i', \\ E_{\parallel 1} &= 0. \end{aligned} \quad \begin{array}{l} \text{conditions for magnetic and} \\ \text{electric fields parallel to ideal} \\ \text{electric surfaces} \end{array} \quad (31)$$

Field components perpendicular to a material boundary

In a very similar way, we can derive the boundary conditions for fields (D_{\perp} , B_{\perp}) that are perpendicular to a boundary surface between two materials. This time, however, we do not define an area but a small cylinder with a volume ΔV around the boundary, as shown in Fig. 8. We form a volume integral from Maxwell's equations (3) and (4) over the volume of the cylinder and apply Gauss's theorem to transform the volume integrals into surface integrals:

$$\int_V \nabla \cdot \mathbf{D} dV = \oint_S \mathbf{D} \cdot d\mathbf{S} = \int_V q_v dV, \quad (32)$$

$$\int_V \nabla \cdot \mathbf{B} dB = \oint_S \mathbf{B} \cdot d\mathbf{S} = 0. \quad (33)$$

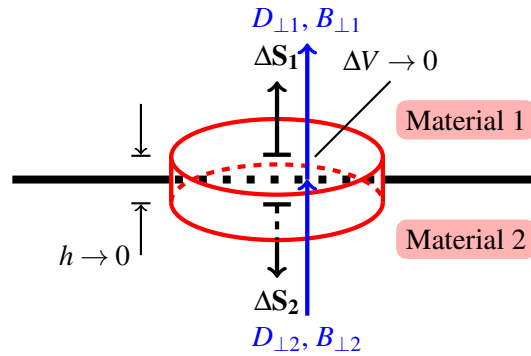


Fig. 8: Boundary conditions perpendicular to a material boundary

In the following step, we reduce the height of the cylinder to zero, so that we end up with two surfaces, one on each side of the boundary. And now it becomes clear why we have to start with a volume integral. Since the surface element $d\mathbf{S}$ is perpendicular to the surface of the cylinder, the 'dot product' in the integrals basically reduces the vector fields \mathbf{D} and \mathbf{B} to the components perpendicular to the surface of the cylinder. This means that above equations can now be written as

$$\begin{aligned} D_{\perp 1} - D_{\perp 2} &= q_s, \\ B_{\perp 1} &= B_{\perp 2}, \end{aligned} \quad \begin{array}{l} \text{conditions for dielectric} \\ \text{displacement and magnetic} \\ \text{induction perpendicular to a} \\ \text{material boundary} \end{array} \quad (34)$$

where q_s is a surface charge (measured in units of C/m^2) that may exist on the boundary surface. In the

case where material 2 is an ideal conductor, we obtain

$$\begin{aligned} D_{\perp 1} &= q_s, \\ B_{\perp 1} &= 0. \end{aligned} \quad \begin{array}{l} \text{conditions for dielectric} \\ \text{displacement and magnetic} \\ \text{induction perpendicular to} \\ \text{ideal electric surface} \end{array} \quad (35)$$

We note that when the fields are parallel to a boundary surface, the electric and magnetic fields are used in the boundary conditions, whereas when they are perpendicular to the boundary surface, we have a condition for the dielectric displacement and the magnetic induction. This means that, for instance, the tangential electric field E_{\parallel} may be smooth across a boundary but there will be a jump in the dielectric displacement D_{\parallel} if there are different relative dielectric constants ϵ_r in the two materials. Similarly, the component of the magnetic induction B_{\perp} perpendicular to a surface may be smooth, whereas the magnetic field H_{\perp} will jump if the two materials have different relative magnetic field constants μ_r .

2 Electromagnetic waves

In this section, we shall derive the general form of the wave equation and then restrict ourselves to phenomena that are harmonic in time. Since RF systems mostly deal with sinusoidal waves, we shall be able to explain and understand most of the relevant phenomena with this approach. This includes the ‘skin effect’, the propagation of energy, RF losses, and acceleration via travelling waves.

2.1 The wave equation

We start with the simplification of looking only at homogeneous, isotropic media, meaning we assume that the electromagnetic fields ‘see’ the same material constants (μ , ϵ , κ) in all directions. With this assumption, Maxwell’s equations can be conveniently expressed in terms of only E and H :

$$\nabla \times \mathbf{H} = \kappa \mathbf{E} + \epsilon \frac{\partial \mathbf{E}}{\partial t}, \quad (36)$$

$$\nabla \times \mathbf{E} = -\mu \frac{\partial \mathbf{H}}{\partial t}, \quad \text{Maxwell's equations} \quad (37)$$

$$\nabla \cdot \mathbf{E} = \frac{q_v}{\epsilon}, \quad (38)$$

$$\nabla \cdot \mathbf{H} = 0. \quad (39)$$

The curl of Eq. (37) together with Eq. (36), and the curl of Eq. (36) together with Eqs. (37) and (38) result in the general wave equations for a homogeneous medium

$$\begin{aligned} \nabla^2 \mathbf{E} - \nabla(\nabla \cdot \mathbf{E}) &= \mu \kappa \frac{d}{dt} \mathbf{E} + \mu \epsilon \frac{d^2}{dt^2} \mathbf{E}, \\ \nabla^2 \mathbf{H} &= \mu \kappa \frac{d}{dt} \mathbf{H} + \mu \epsilon \frac{d^2}{dt^2} \mathbf{H}. \end{aligned} \quad \begin{array}{l} \text{wave equations in a} \\ \text{homogeneous medium} \end{array} \quad (40)$$

In the case of waveguides and cavities, we can simplify these equations even further by considering only the fields inside the waveguide or cavity, which exist in a non-conducting medium ($\kappa = 0$) and a charge-free volume ($\nabla \cdot E = 0$):

$$\begin{aligned} \nabla^2 \mathbf{E} &= \mu \epsilon \frac{d^2}{dt^2} \mathbf{E}, \\ \nabla^2 \mathbf{H} &= \mu \epsilon \frac{d^2}{dt^2} \mathbf{H}. \end{aligned} \quad \begin{array}{l} \text{wave equations in a} \\ \text{non-conducting, charge-free} \\ \text{homogeneous medium} \end{array} \quad (41)$$

2.2 Complex notation for time-harmonic fields

The already compact wave equations in Eq. (41) can be simplified even further by taking into account the fact that in RF engineering one usually deals with time-harmonic signals, which are sometimes modulated in phase or amplitude. We can therefore introduce the complex notation for electric and magnetic fields. We start by assuming a time-harmonic electric field with amplitude E_0 and phase φ ,

$$E(t) = E_0 \cos(\omega t + \varphi), \quad (42)$$

which we can interpret as the real part of a complex expression,

$$E(t) = \Re \{ E_0 e^{i\varphi} e^{i\omega t} \} = \Re \{ E_0 \cos(\omega t + \varphi) + i E_0 \sin(\omega t + \varphi) \}. \quad (43)$$

In this form, we can easily separate the harmonic time dependence ωt from the phase information φ . The phase information can be merged into the amplitude by defining a ‘complex amplitude’ or ‘phasor’

$$\tilde{E} = E_0 e^{i\varphi}. \quad (44)$$

We keep in mind that the real physical fields are obtained as the real part of the complex amplitude times $e^{i\omega t}$:

$$E_0 \cos(\omega t + \varphi) = \Re \{ \tilde{E} e^{i\omega t} \}. \quad (45)$$

To simplify our writing, we skip the part with the harmonic time dependence and omit the tilde, which means that from now on all field quantities are written as complex amplitudes. In order to convince you that this really is a simplification, let us consider what happens to time derivatives when complex notation is used:

$$\frac{d}{dt} \tilde{E} e^{i\omega t} = i\omega \tilde{E} e^{i\omega t}. \quad (46)$$

This means that all time derivatives in Maxwell’s equations and also in the wave equations can simply be replaced by a multiplication by $i\omega$, and we are able to do this because the time dependence is always harmonic. Only when we have to deal with transient events, such as the switching on of an RF amplifier or the sudden arrival of a beam in a cavity, do we have to go back the non-harmonic general equations.

As our first application of the complex notation, we rewrite Maxwell’s equations as follows:

$$\nabla \times \mathbf{H} = i\omega \underline{\epsilon} \mathbf{E}, \quad (47)$$

$$\nabla \times \mathbf{E} = -i\omega \mu \mathbf{H}, \quad \text{Maxwell's equations in} \quad (48)$$

$$\nabla \cdot \mathbf{E} = \frac{\rho_V}{\epsilon}, \quad \text{complex notation} \quad (49)$$

$$\nabla \cdot \mathbf{H} = 0, \quad (50)$$

where the complex dielectric constant $\underline{\epsilon}$ is defined as

$$\underline{\epsilon} = \epsilon' - i\epsilon'' = \epsilon \left(1 - i \frac{\kappa}{\omega \epsilon} \right). \quad \text{complex dielectric constant} \quad (51)$$

We note that $\underline{\epsilon}$ is complex only in a conducting medium. We can now proceed to write the general wave equations in complex form:

$$\nabla^2 \mathbf{E} - \nabla(\nabla \cdot \mathbf{E}) = -k^2 \mathbf{E}, \quad \text{general complex} \quad (52)$$

$$\nabla^2 \mathbf{H} = -k^2 \mathbf{H}. \quad \text{wave equations} \quad (53)$$

Here also, we note that the complex wavenumber \underline{k} becomes real in the case of a non-conducting medium:

$$\underline{k}^2 = \omega^2 \mu \underline{\epsilon} = \omega^2 \mu \epsilon \left(1 - i \frac{\kappa}{\omega \epsilon}\right). \quad \text{complex wavenumber} \quad (54)$$

Finally, we simplify the wave equations again for the case of a non-conducting, charge-free medium and obtain

$$\nabla^2 \mathbf{E} = -k^2 \mathbf{E}, \quad \text{complex wave equations in a non-} \quad (55)$$

$$\nabla^2 \mathbf{H} = -k^2 \mathbf{H}, \quad \text{conducting, charge-free medium} \quad (56)$$

with

$$k^2 = \omega^2 \mu \epsilon = \frac{\omega^2}{c^2}. \quad \text{free-space wavenumber} \quad (57)$$

On the way, we have also introduced a simple definition for the speed of light, $c = 1/\sqrt{\mu\epsilon}$, in Eq. (57).

2.3 Plane waves

As an introduction to the theory of electromagnetic waves, we look at a very simple case, that of so-called plane waves. We assume again that we are in a homogeneous, isotropic, linear medium and that there are no charges or currents, which means that Eqs. (52) and (53) apply. Furthermore—for a plane wave—we assume that the field components depend only on one coordinate (e.g., z). The solution of the harmonic wave equations (52) and (53) can then be written as a superposition of two waves

$$\begin{aligned} E_x(z) &= \underline{C}_1 e^{-\underline{\gamma}z} + \underline{C}_2 e^{+\underline{\gamma}z}, \\ H_y(z) &= \frac{1}{\underline{Z}} (\underline{C}_1 e^{-\underline{\gamma}z} + \underline{C}_2 e^{+\underline{\gamma}z}), \end{aligned} \quad (58)$$

one of which propagates in the positive and one in the negative z direction. The complex propagation constant $\underline{\gamma}$ has a real component α , which describes the damping in a lossy material, and a complex component $i\beta$, which describes the propagation of the wave. The relation between the propagation constant $\underline{\gamma}$ and the wavenumber k is

$$\underline{\gamma} = \alpha + i\beta = i\underline{k} = i\omega\sqrt{\mu\underline{\epsilon}}. \quad \text{propagation constant} \quad (59)$$

We already know that time-harmonic electric and magnetic fields are linked via Maxwell's equations, which means that their amplitudes have a certain fixed ratio to each other. This ratio has been introduced in Eq. (58) as the wave impedance \underline{Z} , the ratio between the electric and magnetic field amplitudes

$$\underline{Z} = \frac{E_y}{H_z} = \sqrt{\frac{\mu}{\underline{\epsilon}}}, \quad \text{complex wave impedance} \quad (60)$$

which becomes real in the absence of lossy material. The wave impedance of free space is given by

$$Z_0 = \sqrt{\frac{\mu_0}{\epsilon_0}} \approx 377 \Omega. \quad \text{free-space wave impedance} \quad (61)$$

2.4 Skin depth

When electromagnetic waves encounter a conducting (lossy) material, we have to evaluate the boundary conditions (see Section 1.5), and we find that the wave amplitudes are attenuated suddenly by an attenuation constant α . In the RF case we can assume that

$$\frac{\kappa}{\omega\epsilon} \gg 1, \quad (62)$$

which means that the complex wavenumber (54) and, obviously, also the complex dielectric constant (51) are dominated by their imaginary parts, so that we can write

$$\underline{\epsilon} \approx -i\epsilon'' = -i\frac{\kappa}{\omega} \quad \text{or} \quad \underline{k}^2 = -i\omega\mu\kappa, \quad (63)$$

which is actually equivalent to neglecting the displacement current. Using Eq. (59), we can then write the propagation constant as

$$\gamma = \alpha + i\beta = i\underline{k} = i\omega\sqrt{\frac{-i\mu\kappa}{\omega}} = (1+i)\sqrt{\frac{\kappa\mu\omega}{2}}, \quad (64)$$

which defines the attenuation constant α . The ‘skin depth’ is then defined as the distance after which the wave amplitudes have been attenuated by a factor $1/e \approx 36.8\%$:

$$\delta_s = \frac{1}{\alpha} = \sqrt{\frac{2}{\omega\mu\kappa}}. \quad \text{skin depth} \quad (65)$$

Knowing the value of the skin depth is crucial for the design of RF equipment. Let us assume that we want to build an accelerating cavity that resonates at 500 MHz. Since high-quality copper is quite expensive, we consider the possibility of constructing the cavity out of steel and then copper-plating the interior in order to obtain a good quality factor and reduce the losses in the surface. From Eq. (65), we calculate that the skin depth in copper is approximately 3 μm . Depending on how well the copper plating is done by the plating company, we can now define the thickness of the copper layer that is needed on the inside of the cavity. Typically, around 10–20 times the skin depth is chosen as the plating thickness. Figure 9 shows the dependence of the skin depth on the RF frequency.

Furthermore, the skin depth allows us to calculate the losses in the surface easily. For a wave travelling parallel to a conducting surface, one can define a surface resistance by assuming a constant current density in a layer of the surface material equivalent to the skin depth, as shown in Fig. 10:

$$R_{\text{surf}} = \frac{1}{\kappa\delta_s} [\Omega]. \quad \text{surface resistance} \quad (66)$$

This value has to be multiplied by l/w to obtain the full RF resistance, where l is the length of the conducting wall and w is its width.

2.5 Energy and transport of energy

We start this section by presenting Poynting’s law, and then explain its components. Poynting’s law states nothing more than the conservation of electromagnetic energy:

$$-\frac{d}{dt} \int_V w dV = \int_A \mathbf{S} \cdot d\mathbf{A} + \int_V \mathbf{E} \cdot \mathbf{J} dV. \quad \text{Poynting’s law} \quad (67)$$

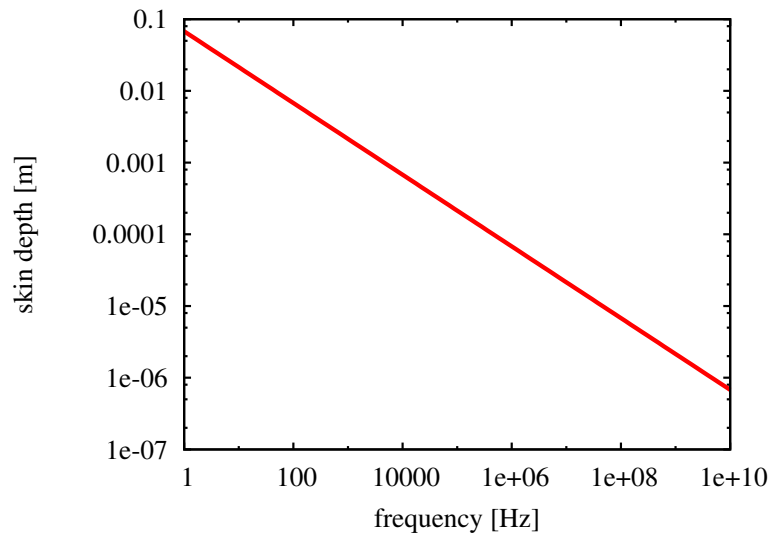


Fig. 9: Skin depth versus RF frequency

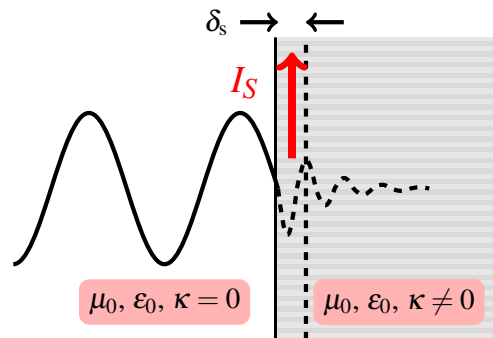


Fig. 10: Skin depth and surface resistance

This equation, read from left to right, states that ‘the rate of change of stored energy in a volume equals the energy flow out of the volume (through a surface \mathbf{A} surrounding the volume) plus the losses within the volume (the work performed on charges per unit time)’. In the following lines, we shall see that the components of Poynting’s law do indeed correspond to what is stated in the previous sentence.

What is $\mathbf{E} \cdot \mathbf{J}$?

In order to understand the expression $\mathbf{E} \cdot \mathbf{J}$, we follow [1] and start with the force acting on a charge moving in an electromagnetic field,

$$\mathbf{F} = q(\mathbf{E} + \mathbf{v} \times \mathbf{B}). \quad \text{Lorentz force} \quad (68)$$

Multiplying this equation by \mathbf{v} and knowing that $\mathbf{a} \cdot (\mathbf{a} \times \mathbf{b}) \equiv 0$, we obtain an expression for the work done on a charge per unit time,

$$\mathbf{v} \cdot \mathbf{F} = q\mathbf{v} \cdot \mathbf{E}. \quad (69)$$

Assuming N particles per unit volume, we can write

$$N\mathbf{v} \cdot \mathbf{F} = Nq\mathbf{v} \cdot \mathbf{E} = \mathbf{J} \cdot \mathbf{E}. \quad (70)$$

Therefore the expression $\mathbf{J} \cdot \mathbf{E}$ must be equal to the work done on charges per unit time and unit volume, or, in other words, the loss of electromagnetic energy per unit volume.

The Poynting vector \mathbf{S} and the energy density w

These quantities can be understood by manipulating Maxwell's equations (compare, e.g., [2]). We multiply Eq. (1) by \mathbf{E} :

$$\mathbf{E} \cdot \mathbf{J} = \mathbf{E} \cdot (\nabla \times \mathbf{H}) - \mathbf{E} \cdot \frac{\partial \mathbf{D}}{\partial t}. \quad (71)$$

Using Eq. (D.1), this can be rewritten as

$$\mathbf{E} \cdot \mathbf{J} = \mathbf{H} \cdot (\nabla \times \mathbf{E}) - \nabla \cdot (\mathbf{E} \times \mathbf{H}) - \mathbf{E} \cdot \frac{\partial \mathbf{D}}{\partial t}. \quad (72)$$

Using the second of Maxwell's equations (2) and assuming time-invariant μ and ϵ , we can write

$$\mathbf{E} \cdot \mathbf{J} = -\nabla \cdot (\mathbf{E} \times \mathbf{H}) - \frac{\partial}{\partial t} \left(\frac{1}{2} \mathbf{E} \cdot \mathbf{D} + \frac{1}{2} \mathbf{H} \cdot \mathbf{B} \right). \quad (73)$$

Applying a volume integral together with Gauss's theorem (16) and rearranging the elements of the equation, we end up with

$$\begin{aligned} -\frac{\partial}{\partial t} \int_V \left(\frac{1}{2} \mathbf{E} \cdot \mathbf{D} + \frac{1}{2} \mathbf{H} \cdot \mathbf{B} \right) dV \\ = \int_A (\mathbf{E} \times \mathbf{H}) \cdot d\mathbf{A} + \int_V \mathbf{E} \cdot \mathbf{J} dV, \end{aligned} \quad \text{Poynting's law} \quad (74)$$

which can be compared directly with Eq. (67). On the left-hand side we have the definition of the energy density,

$$w = w_{\text{el}} + w_{\text{mag}} = \frac{1}{2} \mathbf{E} \cdot \mathbf{D} + \frac{1}{2} \mathbf{B} \cdot \mathbf{H}, \quad \text{electric and magnetic energy density} \quad (75)$$

and from the right-hand side we obtain the definition of the energy flux density, or the Poynting vector \mathbf{S} ,

$$\mathbf{S} = \mathbf{E} \times \mathbf{H}. \quad \text{Poynting vector} \quad (76)$$

The Poynting vector gives us the direction in which an electromagnetic wave transports energy, and from the cross product we understand that this direction is always perpendicular to the electric and magnetic field components. This is consistent with Section 2.3, where we found that the field components (E_x, H_y) of a plane wave (see Eq. (58)) are perpendicular to the direction of propagation (z).

In the above derivation, we have used Maxwell's equations in their general form, meaning with time derivatives. In the case of the complex notation, the definitions of the energy density and Poynting vector have to be modified as follows (for a proof, see [2] or [3]):

$$w = w_{\text{el}} + w_{\text{mag}} = \frac{1}{4} \mathbf{E} \cdot \mathbf{D}^* + \frac{1}{4} \mathbf{B} \cdot \mathbf{H}^*, \quad \text{electric and magnetic energy density in complex notation} \quad (77)$$

$$\mathbf{S} = \frac{1}{2} (\mathbf{E} \times \mathbf{H}^*). \quad \text{complex Poynting vector} \quad (78)$$

3 Electromagnetic waves in waveguides

In this section, we derive the field components of electromagnetic waves that propagate in waveguides. The same principle can then be used to calculate the standing-wave pattern in an accelerating cavity, which is nothing more than a superposition of two waves travelling in opposite directions.

3.1 Classification of modes in waveguides and cavities

Before we start to solve the wave equation, we need to introduce a classification of the field patterns that can be found in waveguides and cavities.

TM_{mnp} modes, or E_{mnp} modes

These modes have no magnetic field in the direction of propagation (z) and are therefore often called *transverse magnetic*, or TM, modes. On the other hand, they have an electric field component that is parallel to z , hence the equivalent name *E modes*.

The indices m, n, p indicate the number of zeros or variations in the three directions of a coordinate system. In the case of a waveguide, only the first two indices are used, whereas in the case of a cavity, owing to the standing-wave pattern along z , all three are needed for a complete description. In the case of a circular waveguide or cavity, the indices indicate the following:

- m , number of full-period variations of the field components in the azimuthal direction. For circularly symmetric geometries, $\mathbf{E}, \mathbf{B} \propto \cos(m\varphi), \sin(m\varphi)$.
- n , number of zeros (x_{mn}) of the axial field component in the radial direction. For circularly symmetric geometries, $E_z, B_z \propto J_m(x_{mn}r/R_c)$.
- p , number of half-period variations of the field components in the longitudinal direction, with $\mathbf{E}, \mathbf{B} \propto \cos(p\pi z/l), \sin(p\pi z/l)$.

The functions J_m introduced above are Bessel functions of the first kind and of m th order, and can be found in mathematical textbooks. The first three orders are shown in Fig. 11.

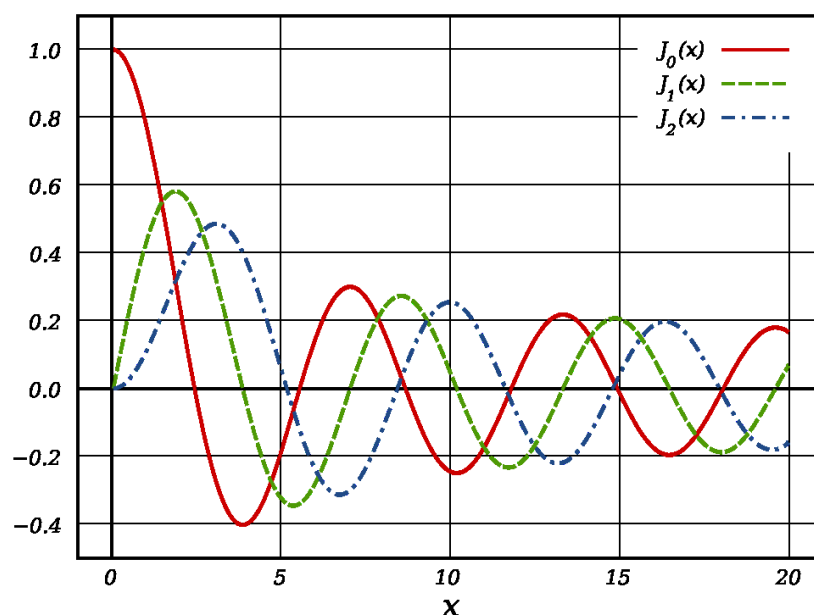


Fig. 11: Bessel functions of the first kind up to order 2

TE_{mnp} modes, or H_{mnp} modes

Here, there is no electric field in the direction of propagation z , hence the name *transverse electric*, or TE, modes. In analogy to the E modes, H modes have a magnetic field component parallel to z . The indices have the same meaning as above.

TEM modes

This class of modes has neither an electric nor a magnetic field component in the direction of propagation. They can exist between two isolated conductors, for example in a coaxial line. The advantage of TEM modes is that waves of any frequency can propagate, whereas TE and TM modes always have a cut-off frequency, below which they are damped exponentially (more on this later). However, the disadvantage of coaxial lines is that the losses in the two conductors are generally higher than in rectangular or circular waveguides.

3.2 Solution of the wave equation in a cylindrical waveguide

Instead of trying to find solutions for all six vector components of the electric and magnetic fields, one can simplify the problem by using a vector potential \mathbf{A} (without any physical meaning) that has only one component. One can then quickly derive all six field components from this vector potential.

It can be shown that only two types of modes can exist in waveguides: TM and TE modes, as introduced above. For each mode type, we introduce a vector potential \mathbf{A} as follows. Since \mathbf{H} and \mathbf{E} are divergence-free, and since $\nabla \cdot (\nabla \times \mathbf{a}) \equiv 0$, we can write

$$\mathbf{H}^{\text{TM}} = \nabla \times \mathbf{A}^{\text{TM}} \quad \text{with} \quad \mathbf{E}^{\text{TM}} = -\frac{i}{\omega\epsilon} \nabla \times (\nabla \times \mathbf{A}^{\text{TM}}), \quad \text{vector potential for TM waves} \quad (79)$$

$$\mathbf{E}^{\text{TE}} = \nabla \times \mathbf{A}^{\text{TE}} \quad \text{with} \quad \mathbf{H}^{\text{TE}} = \frac{i}{\omega\mu} \nabla \times (\nabla \times \mathbf{A}^{\text{TE}}). \quad \text{vector potential for TE waves} \quad (80)$$

In both cases the vector potential obeys the wave equation

$$\nabla^2 \mathbf{A} = -k^2 \mathbf{A} \quad \text{with} \quad k^2 = \omega^2 \mu \epsilon, \quad (81)$$

which can then be solved for various coordinate systems and has only one vector component, in the direction of propagation:

$$\mathbf{A} = A_z \mathbf{e}_z. \quad (82)$$



Fig. 12: Geometry of a circular waveguide

Circular waveguides

In a circular waveguide, as shown in Fig. 12, the vector potentials for the TE and TM modes are identical:

$$A_z^{\text{TM/TE}} = C J_m(k_c r) \cos(m\varphi) e^{\pm i k_z z}, \quad \text{vector potential for circular waveguide} \quad (83)$$

with

$$k_z = \sqrt{k^2 - k_c^2}. \quad \text{wavenumber in } z \text{ direction} \quad (84)$$

Using Eq. (79), we can derive the field components for the TM modes:

$$\left. \begin{aligned} E_r &= \frac{i}{\omega\epsilon} \frac{\partial H_\phi}{\partial z} = -C \frac{k_z k_c}{\omega\epsilon} J'_m(k_c r) \cos(m\phi) \\ E_\phi &= -\frac{i}{\omega\epsilon} \frac{\partial H_r}{\partial z} = C \frac{m k_z}{\omega\epsilon r} J_m(k_c r) \sin(m\phi) \\ E_z &= \frac{i k_c^2}{\omega\epsilon} A_z = C \frac{i k_c^2}{\omega\epsilon} J_m(k_c r) \cos(m\phi) \\ H_r &= \frac{1}{r} \frac{\partial A_z}{\partial \phi} = -C \frac{m}{r} J_m(k_c r) \sin(m\phi) \\ H_\phi &= -\frac{\partial A_z}{\partial r} = -C k_c J'_m(k_c r) \cos(m\phi) \end{aligned} \right\} e^{\pm i k_z z}. \quad \text{field components for TM modes in a circular waveguide} \quad (85)$$

Now we can use the boundary conditions to specify the cut-off wavenumber k_c . From Section 1.5, we know that the electric field components parallel to the waveguide surface have to vanish at the surface, which means

$$\left. \begin{aligned} E_\phi(r=a) &= 0 \\ E_z(r=a) &= 0 \end{aligned} \right\} \Rightarrow J_m(k_c a) = 0 \quad \Rightarrow \quad k_c = \frac{j_{mn}}{a}. \quad (86)$$

The n th zeros j_{mn} of the Bessel functions of order m are tabulated in mathematical textbooks (e.g., [4]).

Using

$$k_c = \frac{2\pi}{\lambda_c} = \frac{\omega_c}{c}, \quad (87)$$

we can define the cut-off frequency of the waveguide,

$$\omega_c = c \frac{j_{mn}}{a}. \quad \text{cut-off frequency for TM modes in a circular waveguide} \quad (88)$$

The mode that is most commonly used in circular waveguides is the TM_{01} mode, which has only three field components. By inserting $m = 0$ and $n = 1$ into Eq. (85) and using $J'_0(r) = -J_1(r)$, we obtain

$$\left. \begin{aligned} E_r &= C \frac{k_z k_c}{\omega\epsilon} J_1(k_c r) \\ E_z &= -C \frac{i k_c^2}{\omega\epsilon} J_0(k_c r) \\ H_\phi &= C k_c J_1(k_c r) \end{aligned} \right\} e^{\pm i k_z z}, \quad \text{field components of } \text{TM}_{01} \text{ mode in a circular waveguide} \quad (89)$$

with a cut-off frequency $\omega_c \approx c \times (2.405/a)$.

The field pattern of the TM_{01} mode is shown in Fig. 13 for a mode frequency 15% above the cut-off frequency. The distance between the minima or between the maxima of the field corresponds to 0.5 times the propagation wavelength λ_z . With decreasing mode frequency, $\lambda_z = 2\pi/k_z$ becomes longer, and finally becomes infinite when the mode frequency equals the cut-off frequency ω_c . This effect is shown in Fig. 14, where the TM_{01} mode propagates at a frequency just 0.5% above the cut-off frequency.

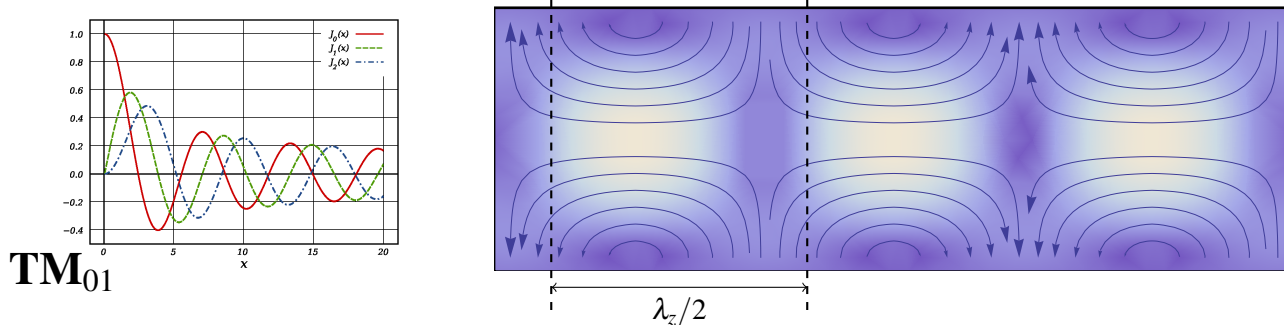


Fig. 13: Field lines of a TM_{01} mode in a circular waveguide with $\omega = 1.15\omega_c$. Solid lines, electric field lines; dashed lines, magnetic field lines. The brightness of the background is proportional to the norm of the field vector: light areas indicate high-field regions of the magnetic field in the left plot and of the electric field in the right plot.

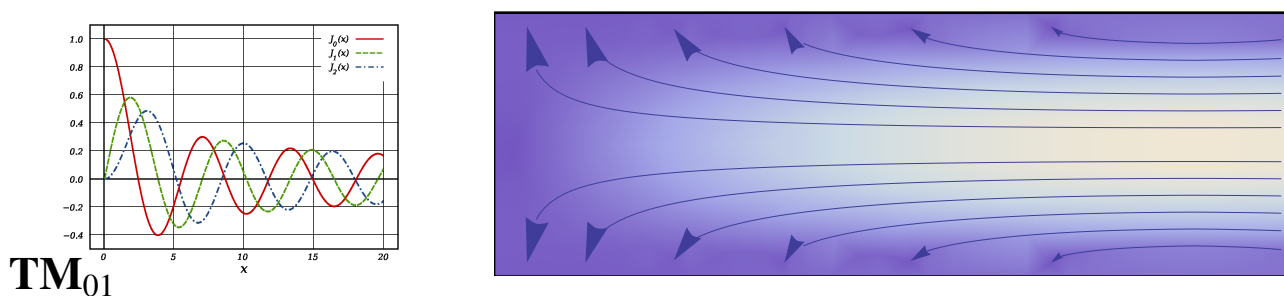


Fig. 14: Field lines of a TM_{01} mode in a circular waveguide with $\omega = 1.005\omega_c$. Solid lines, electric field lines; dashed lines, magnetic field lines. The brightness of the background is proportional to the norm of the field vector: light areas indicate high-field regions of the magnetic field in the left plot and of the electric field in the right plot.

Rectangular waveguides

The derivation of the fields in a rectangular waveguide follows the same principle as that used in the previous section for circular waveguides. In a rectangular waveguide, as shown in Fig. 15, two different vector potentials are needed to describe the TE and TM modes:

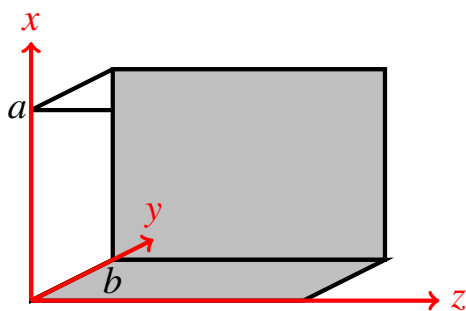


Fig. 15: Geometry of a rectangular waveguide with transverse dimensions a and b

$$A_z^{\text{TM}} = C \sin(k_x x) \sin(k_y y) e^{\pm i k_z z},$$

**vector potential for TM waves
in a rectangular waveguide** (90)

$$A_z^{\text{TE}} = C \cos(k_x x) \cos(k_y y) e^{\pm i k_z z}, \quad \text{vector potential for TE waves in a rectangular waveguide} \quad (91)$$

where

$$k_z = \sqrt{k^2 - k_c^2}, \quad \text{with} \quad k_c^2 = k_x^2 + k_y^2. \quad \text{wavenumber in z direction} \quad (92)$$

We note that the position of the origin of the coordinate system is linked to the sine and cosine terms in Eqs. (90) and (91). The fields derived from the vector potentials have to fulfil the boundary conditions on the waveguide walls. So if, for instance, we were to choose the origin in the centre of the waveguide, then the sine and cosine expressions would have to be exchanged to account for the changed symmetries with respect to the coordinate axes. Using Eq. (79) again, we derive the field components for the TM modes:

$$\left. \begin{aligned} E_x &= \frac{i}{\omega \epsilon} \frac{\partial H_y}{\partial z} = \pm C \frac{k_z}{\omega \epsilon} \cos(k_x x) \sin(k_y y) \\ E_y &= -\frac{i}{\omega \epsilon} \frac{\partial H_x}{\partial z} = \pm C \frac{k_z}{\omega \epsilon} \sin(k_x x) \cos(k_y y) \\ E_z &= \frac{i(k_z^2 - k^2)}{\omega \epsilon} A_z^{\text{TM}} = C \frac{i(k_z^2 - k^2)}{\omega \epsilon} \sin(k_x x) \sin(k_y y) \\ H_x &= \frac{\partial A_z^{\text{TM}}}{\partial y} = C k_y \sin(k_x x) \cos(k_y y) \\ H_y &= -\frac{\partial A_z^{\text{TM}}}{\partial x} = -C k_x \cos(k_x x) \sin(k_y y) \end{aligned} \right\} e^{\pm i k_z z}. \quad \text{field components for TM modes in a rectangular waveguide} \quad (93)$$

Using the boundary conditions, we can specify the wavenumbers k_x and k_y :

$$\left. \begin{aligned} E_y(x=a) &= 0 \\ E_z(x=a) &= 0 \end{aligned} \right\} \Rightarrow k_x = \frac{m\pi}{a} \quad \text{and} \quad m = 0, 1, 2, \dots, \quad (94)$$

$$\left. \begin{aligned} E_x(y=b) &= 0 \\ E_z(y=b) &= 0 \end{aligned} \right\} \Rightarrow k_y = \frac{n\pi}{b} \quad \text{and} \quad n = 0, 1, 2, \dots, \quad (95)$$

and the cut-off frequency for a rectangular waveguide is

$$\omega_c = c k_c = c \sqrt{k_x^2 + k_y^2} = c \pi \sqrt{\left(\frac{m}{a}\right)^2 + \left(\frac{n}{b}\right)^2}. \quad \text{cut-off frequency for TM modes in a rectangular waveguide} \quad (96)$$

The usual convention is to have $a > b$, and in this case the TE_{10} mode is the mode with the lowest cut-off frequency. It is also the only mode that propagates in a relatively large frequency band, from $f_c^{\text{TE},10}$ to $2f_c^{\text{TE},10}$, which is why it is the mode most commonly used in rectangular waveguides. The fields of the TE modes can be derived from the TE vector potential using the same procedure.

3.3 Wave propagation and dispersion relation

In Figs. 13 and 14, we have seen that the propagation wavelength λ_z of a waveguide mode is determined by its frequency and by how far the mode frequency is above the cut-off frequency of the waveguide. If the propagation wavelength depends on the mode frequency, we can assume that the phase velocity of a particular mode also depends on the mode frequency. This relationship is called the dispersion relation and, using the definition of the wavenumber in Eq. (84), we can write

$$k_z^2 = k^2 - k_c^2 = \frac{\omega^2 - \omega_c^2}{c^2} = \frac{\omega^2}{v_{\text{ph}}^2}, \quad \text{dispersion relation} \quad (97)$$

from which we can immediately see that:

- k_z can be real only if the mode frequency ω is above the cut-off frequency ω_c ;
- for $\omega < \omega_c$, the mode cannot propagate and the fields are exponentially damped.

We also have a definition of the phase velocity, which is the speed at which the maxima and minima of the field patterns move along the waveguide:

$$v_{\text{ph}} = \frac{\omega}{k_z} = c^2 \frac{\omega^2}{\omega^2 - \omega_c^2}. \quad \text{phase velocity} \quad (98)$$

This is not to be confused with the speed with which the wave actually propagates in the waveguide. The dispersion relation is usually plotted in the form of a ‘Brillouin diagram’, as shown in Fig. 16.

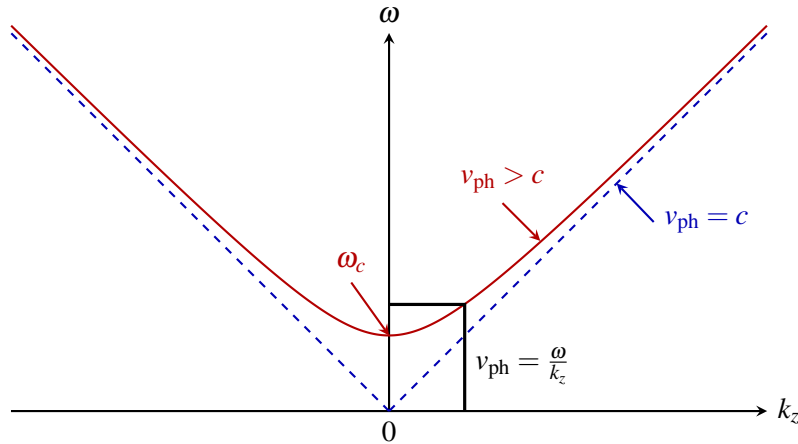


Fig. 16: Dispersion relation in a waveguide. The dotted line shows the case $v_{\text{ph}} = c$.

The slope of the dispersion relation is the group velocity

$$v_{\text{gr}} = \frac{d\omega}{dk_z}, \quad \text{group velocity} \quad (99)$$

which gives the velocity with which a signal or energy is transported along the waveguide. From Fig. 16, we can conclude that:

- Each frequency has a certain phase velocity and group velocity, which means that signals with a frequency bandwidth will become deformed while travelling along a waveguide. With the help of the dispersion relation, we can easily quantify how much deformation will occur.
- The phase velocity v_{ph} is always larger than the velocity of light c , and at cut-off ($\omega = \omega_c$) it even becomes infinite ($k_z = 0$ and $v_{\text{ph}} \rightarrow \infty$).
- For acceleration, one needs synchronism between the phase velocity (the speed of the field pattern) and the velocity of the particles, which implies that acceleration in waveguides is impossible.
- Information and therefore energy travel at the group velocity, which is always slower than the speed of light.

3.4 Attenuation of waves (power loss method)

Up to this point, we have assumed perfect electrical conductors as the boundaries of our waveguides. Real waveguides and cavities have a certain resistance, and the fields therefore penetrate into the conductors, which significantly complicates the solution of the wave equation. However, we have seen in Section 2.4 that the skin depth in metals is very much smaller than the RF wavelength. This means that we can reasonably assume that the field patterns in a waveguide with ideal boundaries and in a waveguide with resistive metal boundaries will be practically identical (of course, only for good conductors such as copper or aluminium). In order to calculate the attenuation of waves, we can therefore use the fields of a waveguide with ideal electrical boundaries. From the magnetic field, we calculate the induced current in the waveguide walls, and then apply the resistance of the real material to calculate the losses and then the damping of the wave. This principle is called the power loss method and is a simplified method for calculating RF losses on the surfaces of good conductors.

We start by defining the power that is lost per unit length along the longitudinal axis of the waveguide,

$$P' = -\frac{dP}{dz}. \quad (100)$$

From

$$E, H \propto e^{-\alpha z} \quad \Rightarrow \quad P \propto e^{-2\alpha z}, \quad (101)$$

we immediately obtain

$$P' = -\frac{dP}{dz} = 2\alpha P \quad (102)$$

and thus the definition of the attenuation constant

$$\alpha = \frac{P'}{2P}. \quad \text{attenuation constant} \quad (103)$$

In the next steps, we need to derive expressions for the power P transported through the waveguide, and the power loss per unit length P' . Using the field components of the TM_{01} mode given in Eq. (89) and the definition of the complex Poynting vector in Eq. (78), we obtain

$$P = \frac{1}{2} \int_A (\mathbf{E} \times \mathbf{H}^*) \cdot d\mathbf{A} = \frac{1}{2} \int_0^a \int_0^{2\pi} E_r H_\phi^* r dr d\phi = \frac{C^2 k_z k_c^2 \pi a^2 J_1^2(k_c a)}{\omega \epsilon}, \quad (104)$$

where we have used

$$\int_0^a J_1^2(k_c r) r dr = \frac{a^2}{2} J_1^2(k_c a). \quad (105)$$

In order to calculate the losses on the waveguide surface, we first need to know the surface currents that flow within the skin depth. For this purpose, we make use of Ampère's law, as shown in Fig. 17:

$$\oint_c \mathbf{H} \cdot d\mathbf{l} = I = \oint_c \mathbf{J} \cdot (\delta_s d\mathbf{l}). \quad \text{Ampère's law} \quad (106)$$

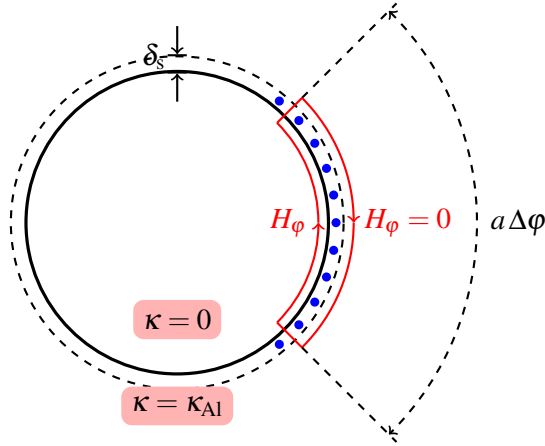


Fig. 17: Ampère's law applied to calculate the surface currents in a circular waveguide

Since the magnetic field has only an azimuthal component, we obtain

$$H_\phi(r = a, z) = Ck_c J_1(k_c a) e^{-ik_z z} = J_z(z) \delta_s. \quad (107)$$

The power density (in W/m³) in the waveguide wall is given by

$$p_v = \frac{1}{2} \mathbf{E} \cdot \mathbf{J}^* = \frac{1}{2\kappa} J_z J_z^* = \frac{\partial^3 P}{(\partial r)(r \partial \phi)(\partial z)}, \quad \text{power density} \quad (108)$$

from which we can write an expression for the power loss per unit length. Together with Eq. (107), we obtain

$$P' = \frac{\partial P}{\partial z} = \int_a^{a+\delta_s} \int_0^{2\pi} p_v r dr d\phi = \frac{\pi a C^2 k_c^2 J_1^2(k_c a)}{\kappa \delta_s}, \quad \text{power loss per unit length} \quad (109)$$

where we have used the fact that $\delta_s \ll a$ to simplify the evaluation of the integral. Now we insert Eqs. (104) and (109) into Eq. (103) and obtain an expression for the attenuation of a TM₀₁ mode in a circular waveguide,

$$\alpha = \frac{P'}{2P} = \frac{R_{\text{surf}}}{Z_0 a \sqrt{1 - (f_c/f)^2}}. \quad \text{attenuation of TM}_{01} \text{ mode in circular waveguide} \quad (110)$$

In the expression above, we have used the definition of the surface resistance given in Eq. (66) and the definition of the free-space wave impedance Z_0 given in Eq. (61).

As an example, we have plotted the attenuation constant for an aluminium waveguide in Fig. 18, where we can see that for this type of waveguide:

- Large-diameter waveguides result in smaller losses, which means that a cost optimum has to be found between the cost of the waveguide, its space requirements, and the losses.
- The minimum losses occur when the operating frequency of the TM₀₁ mode is a factor of $\sqrt{3}$ above the cut-off frequency (try to prove this!).

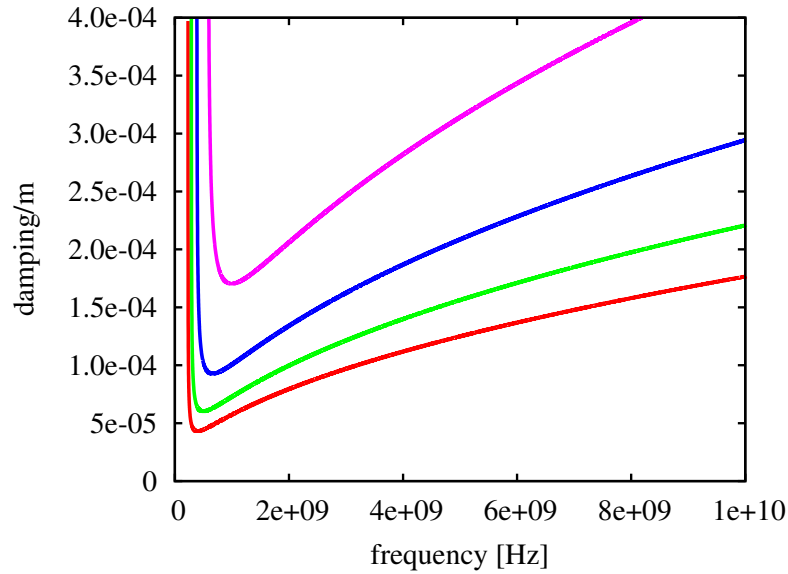


Fig. 18: Attenuation of the TM_{01} mode in a circular aluminium waveguide for several different radii: bottom to top, 0.5 m, 0.4 m, 0.3 m, 0.2 m

4 Accelerating cavities

4.1 Travelling-wave cavities

In order to accelerate particles in a ‘waveguide-like’ structure, the phase velocity in the structure needs to be slowed down, which can be achieved by putting some ‘obstacles’ into the waveguide. In Fig. 19, we see a simple example of a disc-loaded waveguide.

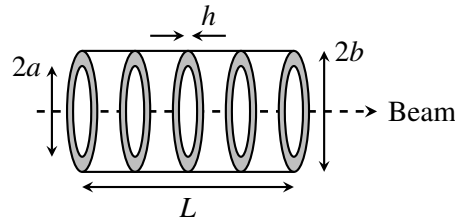


Fig. 19: Geometry of a simple travelling-wave structure

The dispersion relation for such a structure is derived in, for example, [5] as

$$\omega = \frac{2.405c}{b} \sqrt{1 + \kappa(1 - \cos(k_z L)e^{-\alpha h})}, \quad \text{dispersion relation of disc-loaded circular waveguide} \quad (111)$$

where

$$\kappa = \frac{4a^3}{3\pi J_1^2(2.405)b^2 L} \ll 1 \quad \text{and} \quad \alpha \approx \frac{2.405}{a}. \quad (112)$$

Plotting Eq. (111) gives us the Brioullin diagram in Fig. 20, where we can see that we now obtain phase velocities that are equal to or even below the speed of light. We can also understand why the $2\pi/3$ mode is often used for acceleration in electron accelerators, because for this mode (in this example) the phase velocity is just equal to the speed of light. It should be noted that with different geometries, it is possible to operate with different modes and also at velocities $v_{ph} < c$. When a structure operates in the $2\pi/3$

mode, this means that the RF phase shifts by $2\pi/3$ per cell, or, in other words, one RF period extends over three cells.

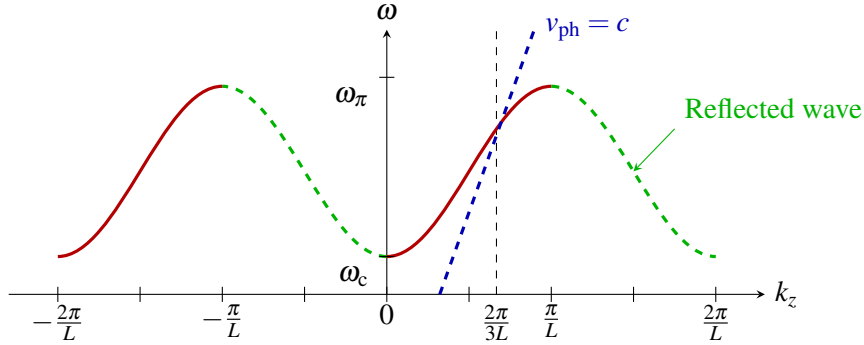


Fig. 20: Dispersion diagram for a disc-loaded travelling-wave structure. Here, the chosen operating point is $v_{\text{ph}} = c$ and $k_z = 2\pi/3L$.

By attaching an input and an output coupler to the outermost cells of the structure, we obtain a usable accelerating structure. Since the particles gain energy in every cell, the electromagnetic wave becomes increasingly damped along the structure. It is then extracted via the output coupler and dumped in an RF load. If one is interested in obtaining the maximum possible accelerating gradient in each cell, then one can counteract the decreasing fields by changing the bore radius from cell to cell. The idea is to slow down the group velocity from cell to cell and obtain a ‘constant-gradient’ structure, rather than a ‘constant-impedance’ structure where the bore radius is kept constant. Other optimizations, for example for maximum efficiency, are also possible.

4.2 Standing-wave cavities

One obtains a cylindrical standing-wave structure by simply closing both ends of a circular waveguide with electric walls. This yields multiple reflections on the end walls until a standing-wave pattern is established. Owing to the additional boundary conditions in the longitudinal direction, we obtain another ‘restriction’ on the existence of electromagnetic modes in the structure. Whereas a longitudinally open travelling-wave structure allows all frequencies and all cell-to-cell phase variations on the dispersion curve, now only certain ‘loss-free’ modes (still assuming perfectly conducting walls) with discrete frequencies and discrete phase changes can exist in a cavity. If RF power is fed in at a different frequency, then the fields excited are damped exponentially, similarly to the modes below the cut-off frequency of a waveguide.

The corresponding dispersion relation for a standing-wave cavity can again be found in textbooks (see [5] and also [6]). However, it is necessary to pay attention to whether the structure under consideration has magnetic or electric cell-to-cell coupling and what kind of end cell is assumed in the analysis. The most common form of the dispersion relation is derived from a coupled-circuit model with $N + 1$ cells. Usually the model has half-cell terminations on both ends of the chain, representing the behaviour of an infinite chain of electrically coupled resonators (compare the original paper by Nagle *et al.* [7]):

$$\omega_n = \frac{\omega_0}{\sqrt{1 + k \cos(n\pi/N)}}, \quad n = 0, 1, \dots, N. \quad \text{dispersion relation for half-cell-terminated standing-wave structure} \quad (113)$$

Assuming an odd number of cells, ω_0 is the frequency of the $\pi/2$ mode and of an uncoupled single cell; k is the cell-to-cell coupling constant, and $n\pi/N$ is the phase shift from cell to cell. For $k \ll 1$, which is usually fulfilled, the coupling constant is given by

$$k = \frac{\omega_{\pi \text{ mode}} - \omega_{0 \text{ mode}}}{\omega_0} \quad \text{coupling constant} \quad (114)$$

Two characteristics of the dispersion curve are worth noting:

- The total width of the frequency band of the mode, $\omega_{\pi \text{ mode}} - \omega_{0 \text{ mode}}$, is independent of the number of cells, which means that we can determine the cell-to-cell coupling constant by measuring the complete structure (but this is only true if all coupling constants are equal).
- For electric coupling, the 0 mode has the lowest frequency and the π mode has the highest. In the case of magnetic coupling, this behaviour is reversed, and one can find the corresponding dispersion curve by changing the sign before the coupling constant in Eq. (113).

In Fig. 21, we plot the dispersion curve for a seven-cell (half-cell-terminated) magnetically coupled structure according to Eq. (113).

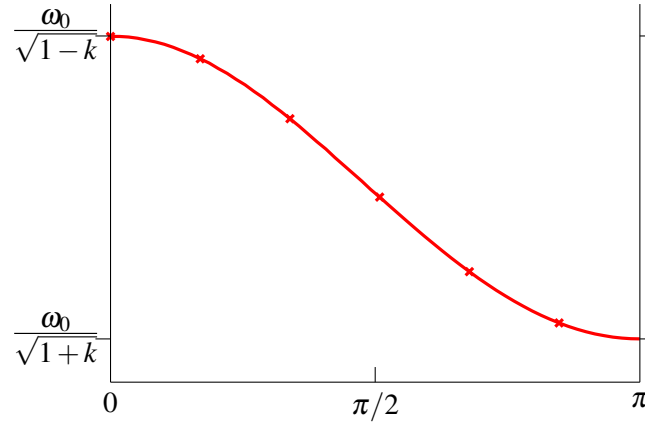


Fig. 21: Dispersion diagram for a standing-wave structure with seven magnetically coupled cells

In practice, one usually has cavities with full-cell termination, and in this case one has to detune the frequencies of the end cells to obtain a flat field distribution in the cavity [8]. In this case it is possible to have a flat field distribution for either the 0 mode or the π mode but not for both at the same time, because the end cells have to be detuned by different amounts in the two cases [9].

4.3 Standing wave versus travelling wave

The principal difference between the two types of cavity is in how and how fast the cavities are filled with RF power. Travelling-wave structures are filled ‘in space’, which means that, basically, cell after cell is filled with power. For the following estimations, we assume a frequency in the range of hundreds of megahertz. The filling of a travelling-wave structure typically takes place with a speed of approximately 1–3% of the speed of light and results in total filling times in the submicrosecond range. Standing-wave structures, on the other hand, are filled ‘in time’: the electromagnetic waves are reflected at the end walls of the cavity and slowly build up a standing-wave pattern of the desired amplitude. For normal-conducting cavities, the time required for this process is typically in the range of tens of microseconds. For superconducting cavities, the filling time can easily go into the millisecond range (depending on the required field level, the accelerated current, and the cavity parameters). This means that for applications that require very short beam pulses ($< 1 \mu\text{s}$), travelling-wave structures are much more power-efficient. For longer pulses ($> n \times 10 \mu\text{s}$), both types of structures can be optimized to achieve similar efficiencies and costs.

Since one can have extremely short RF pulses in a travelling-wave structure, one can obtain much higher peak fields than in a standing-wave structure. This is demonstrated by the accelerating structures for CLIC [10], which have reached values of approximately 100 MV/m (limited by electrical breakdown), whereas the design gradient for the superconducting (standing-wave) cavities for the ILC [11] is just slightly above 30 MV/m (this value is generally limited by field emission and by quenches caused by the peak magnetic field).

Travelling-wave structures can, theoretically, be designed for non-relativistic particles. In existing accelerators, however, they are mostly used for relativistic particles. Low-beta acceleration is typically performed with standing-wave cavities.

Because of the lack of an obvious criterion (other than the pulse length or the particle velocity), an optimization and costing exercise has to be performed for each specific application in order to decide which structure is more efficient. Two excellent papers [12, 13] in which this exercise is performed can be used as references.

4.4 The pillbox cavity

In this chapter, we shall analyse only the simplest TM-mode cavity, the so-called pillbox cavity. A selection of cavities using other mode types is described in [14].

Resonating cavities can be represented conveniently by a lumped-element circuit consisting of an inductor (for storage of magnetic energy) and a capacitor (for storage of electric energy). Looking at Fig. 22, one can easily imagine how the lumped circuit can be transformed into a cavity.

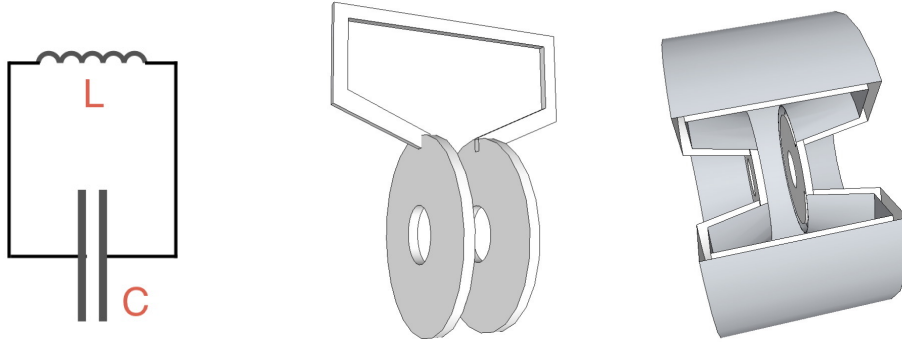


Fig. 22: Transition from a lumped resonating circuit to a resonating cavity

The pillbox cavity is nothing more than an empty cylinder with a conducting inner surface. The simplest mode in this cavity is the TM_{010} mode, which has zero full-period variations in the azimuthal direction (φ), one ‘zero’ of the axial field component in the radial direction (r), and zero half-period variations in the longitudinal (z) direction. We can derive the general field equations by using the vector potential for a circular waveguide given in Eq. (83) and simply superimposing two waves, one propagating in the positive z direction and one in the negative z direction:

$$A_z^{TM/TE} = CJ_m(k_r r) \cos(m\varphi) \underbrace{\left(e^{-ik_z z} + e^{ik_z z} \right)}_{2 \cos(k_z z)}. \quad \text{vector potential for travelling waves in the positive and negative } z \text{ directions} \quad (115)$$

Using Eq. (79), we derive the TM field components

$$\begin{aligned}
E_r &= \frac{i}{\omega\epsilon} \frac{\partial H_\phi}{\partial z} = i2C \frac{k_z k_r}{\omega\epsilon} J'_m(k_r r) \cos(m\phi) \sin(k_z z), \\
E_\phi &= -\frac{i}{\omega\epsilon} \frac{\partial H_r}{\partial z} = -i2C \frac{m k_z}{\omega\epsilon r} J_m(k_r r) \sin(m\phi) \sin(k_z z), \\
E_z &= \frac{i k_r^2}{\omega\epsilon} A_z = i2C \frac{k_r^2}{\omega\epsilon} J_m(k_r r) \cos(m\phi) \cos(k_z z), \\
H_r &= \frac{1}{r} \frac{\partial A_z}{\partial \phi} = -2C \frac{m}{r} J_m(k_r r) \sin(m\phi) \cos(k_z z), \\
H_\phi &= -\frac{\partial A_z}{\partial r} = -2C k_r J'_m(k_r r) \cos(m\phi) \cos(k_z z).
\end{aligned}
\tag{116}$$

TM modes in a pillbox cavity

In the case of standing-wave cavities, the term ‘cut-off’ frequency does not really make sense, so we have replaced the symbol k_c by k_r , indicating that we have a radial dependence of the axial field component, which can also be interpreted as a radial wavenumber.

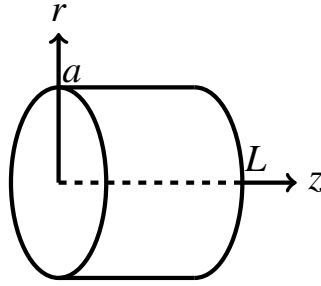


Fig. 23: Pillbox cavity

In the next step, we apply the boundary conditions for a pillbox with radius a and length L as shown in Fig. 23. We obtain

$$E_r(z=0/L), E_\phi(z=0/L) = 0 \quad \Rightarrow k_z = \frac{p\pi}{L}, \tag{117}$$

$$E_\phi(r=a), E_z(r=a), H_r(r=a) = 0 \quad \Rightarrow k_r = \frac{j_{mn}}{a}. \tag{118}$$

In the case of the circular waveguide, the transverse boundary condition made a discrete quantity out of k_c (which we now call k_r in the above equations), and thus defined the cut-off frequency. Now, with the second boundary in the z direction, we obtain a discrete solution for k_z also. The two boundary conditions together result in a discrete set of frequencies (the dispersion relation) for our pillbox cavity:

$$k^2 = \frac{\omega^2}{c^2} = k_z^2 + k_r^2 \quad \Rightarrow f_{mnp}^{\text{TM}} = \frac{c}{2\pi} \sqrt{\left(\frac{j_{mn}}{a}\right)^2 + \left(\frac{p\pi}{L}\right)^2}. \tag{119}$$

dispersion relation for TM modes in a pillbox cavity

We note that the dispersion relation of a single-cell cavity as given above is different from the dispersion relation that can be derived for a multicell cavity, as in the case of Eq. (113). The latter is derived from a model of equivalent lumped circuits, each representing a cell resonating in the TM_{010} mode and coupled to its neighbours in order to model the behaviour of a multicell cavity, whereas Eq. (119) is directly derived from Maxwell’s equations and describes a field pattern that is created by the boundary conditions of our pillbox.

The TM mode with the lowest frequency is the TM_{010} mode, with a frequency

$$f_{010}^{\text{TM}} = \frac{2.405c}{2\pi a}, \quad \text{frequency of the TM}_{010} \text{ pillbox mode} \quad (120)$$

and its field components are

$$\begin{aligned} E_z &= -i2C \frac{j_{01}^2}{a^2 \omega \epsilon} J_0 \left(\frac{j_{01} r}{a} \right) = E_0 J_0 \left(\frac{j_{01} r}{a} \right), \\ H_\phi &= 2C \frac{j_{01}}{a} J_1 \left(\frac{j_{01} r}{a} \right) = \frac{E_0}{Z_0} J_1 \left(\frac{j_{01} r}{a} \right). \end{aligned} \quad \text{field components of the TM}_{010} \text{ pillbox mode} \quad (121)$$

Figure 24 shows the field pattern of the TM_{010} mode, simulated by Superfish[®].

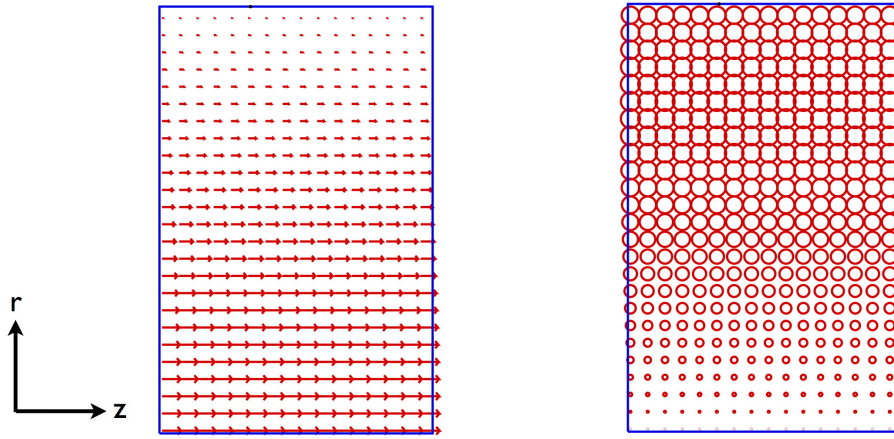


Fig. 24: Field pattern of the TM_{010} mode in a pillbox cavity

4.5 Basic cavity parameters

In order to characterize and optimize cavities, we need some commonly used figures of merit, which we shall define here in general terms and then apply to our simple pillbox cavity. In the following, we assume that we are dealing with an axially symmetric cavity resonating in the TM_{010} mode.

4.5.1 Energy gain in a cavity

For particles traversing a cavity on axis, the electric field generally has the following form:

$$E_z(r=0, z, t) = E(0, z) \cos(\omega t + \varphi), \quad (122)$$

which we can use to calculate the energy gain of a particle when it traverses the cavity,

$$\begin{aligned} \Delta W &= q \int_{-L/2}^{L/2} E(0, z) \cos(\omega t + \varphi) \\ &= qV_0 T \cos \varphi = qE_0 T L \cos \varphi, \end{aligned} \quad \text{energy gain in a cavity (Panofsky equation)} \quad (123)$$

where the cavity voltage is given by

$$V_0 = \int_{-L/2}^{L/2} E(0, z) dz = E_0, \quad \text{cavity voltage} \quad (124)$$

and the ‘difficult mathematics’ has been lumped into the so-called transit time factor

$$T = \frac{\int_{-L/2}^{L/2} E(0, z) \cos(\omega t(z)) dz}{\int_{-L/2}^{L/2} E(0, z) dz} - \tan \phi \underbrace{\frac{\int_{-L/2}^{L/2} E(0, z) \sin(\omega t(z)) dz}{\int_{-L/2}^{L/2} E(0, z) dz}}_{=0 \text{ if } E(0, z) \text{ is symmetric about } z=0}. \quad \text{transit time factor} \quad (125)$$

This takes into account the fact that the RF electric field changes during the passage of the particles. It gives the ratio between the energy gained in an RF field and in a DC field and is therefore always less than 1. We note that the Panofsky equation takes account of the changing velocity of the particles when they cross the accelerating gap. This makes the integrals in the above equations difficult to evaluate. Assuming that the velocity change of the beam particles during their passage is small, however, one can say that

$$\omega t \approx \omega \frac{z}{v} = \frac{2\pi z}{\beta \lambda}, \quad (126)$$

which changes the expression for the transit time factor to (assuming that $E(0, z)$ is symmetric about $z = 0$)

$$T = \frac{\int_{-L/2}^{L/2} E(0, z) \cos(2\pi z / \beta \lambda) dz}{\int_{-L/2}^{L/2} E(0, z) dz}. \quad \text{transit time factor for small velocity changes} \quad (127)$$

The accelerating voltage V_{acc} is the voltage that the particle ‘sees’ when crossing the cavity and should not be confused with the cavity voltage V_0 . We thus define

$$V_{\text{acc}} = V_0 T = E_0 L T. \quad \text{accelerating voltage} \quad (128)$$

4.5.2 Shunt impedance

The shunt impedance tells us how much voltage a cavity will provide when a certain amount of power is dissipated in the cavity walls. This is one of the parameters to be maximized in cavity design, since a large shunt impedance reduces the power consumption of an RF cavity. The general definition is

$$R_s = \frac{V_0^2}{P_d}. \quad \text{shunt impedance (linac definition)} \quad (129)$$

The benefit of a high shunt impedance can easily be diminished by having a small transit time factor, because in this case the cavity voltage cannot be used efficiently to transfer energy to the beam. Therefore one usually tries to optimize both the shunt impedance and the transit time factor, which explains the

definition of the effective shunt impedance

$$R = \frac{(V_0 T)^2}{P_d} \quad \text{effective shunt impedance} \quad (130)$$

When comparing multicell structures operating at different frequencies, one is interested less in the efficiency per cell (because the cell size depends on, for instance, the frequency chosen) than in the efficiency per unit length of the accelerating structure. For this reason, we define

$$Z = \frac{R_s}{L} = \frac{E_0^2}{P_d/L} \quad \text{shunt impedance per unit length} \quad (131)$$

and

$$ZT^2 = \frac{R}{L} = \frac{(E_0 T)^2}{P_d/L} \quad \text{effective shunt impedance per unit length} \quad (132)$$

4.5.3 'Linac' and 'circuit' definitions of shunt impedance

It turns out that different communities of accelerator experts use different definitions of the shunt impedance. Linac experts usually use the definitions presented above, whereas the people who deal with circular machines generally use a definition that is derived from the lumped-circuit definition of a resonator (see Section 4.7). In that definition, all shunt impedances are exactly half as large, following

$$R_s^c = \frac{V_0^2}{2P_d} \quad \text{shunt impedance (circuit definition)} \quad (133)$$

So, before you discuss shunt impedances with anyone, make sure that you are using the same definition. In order to mark the difference clearly, we use R_s^c in this text to identify when the circuit definition is being used.

4.5.4 3 dB bandwidth and quality factor

The quality factor Q describes the bandwidth of a resonator and is defined as the ratio of the reactive power (stored energy) to the real power that is lost in the cavity walls:

$$Q = \frac{\omega}{\Delta\omega} = \frac{\omega W}{P_d} \quad \text{quality factor} \quad (134)$$

If a resonator were built with ideal electrical walls (zero electrical resistance), the resonance curve would be a delta function at the resonance frequency. So, the bandwidth $\Delta\omega$ would be zero and the quality factor would be infinite. In reality, even superconducting cavities have a certain surface resistance, which is why all our cavities have a certain bandwidth and a finite quality factor. Figure 25 shows a typical resonance curve measured with a network analyser. In a measurement of this kind, two antennas penetrate the cavity. The first antenna sends an RF signal with a frequency sweep, and the second picks up the field level in the cavity. As a result, we obtain a plot of the field level versus frequency. The bandwidth is defined as the frequency width of the resonance curve, measured as the distance between the points where the field level has dropped by 50% (or -3 dB), as shown in Fig. 25.

Together with the shunt impedance, one can define another figure of merit, (R/Q) , which is used to maximize the energy gain in a cavity for a given stored energy:

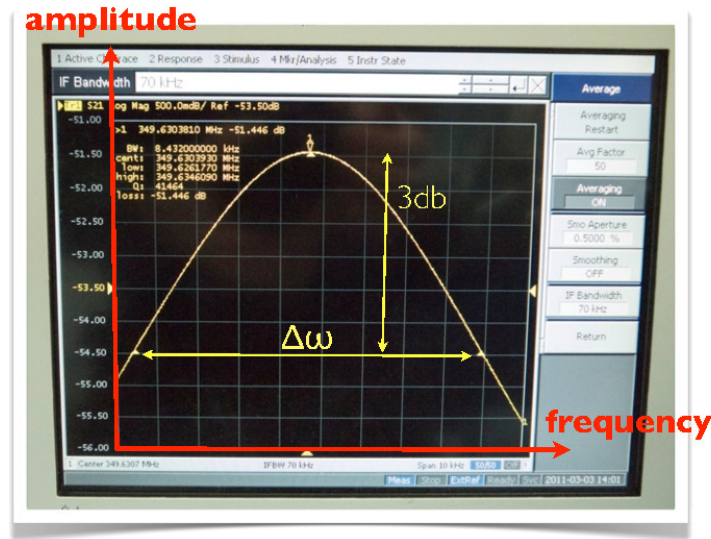


Fig. 25: Measurement of frequency, 3 dB bandwidth, and Q-factor with a network analyser

$$\left(\frac{R}{Q}\right) = \frac{(V_0 T)^2}{\omega W} \quad (R/Q) \quad (135)$$

(R/Q) is independent of the surface losses of the cavity and can therefore be used to qualify the geometry of an accelerating cavity.

4.5.5 Filling time of a cavity

This section is a short extract from [14], which can be consulted for more details. The dissipated power in a cavity must be equal to the rate of change of the stored energy:

$$P_d = -\frac{dW}{dt} = \frac{\omega_0 W}{Q_0} \quad (136)$$

The solution of the above equation can be written as

$$W(t) = W_0 e^{-2t/\tau}, \quad (137)$$

which describes an exponential decay of the stored energy with a ‘filling time constant’ τ , where

$$\tau = \frac{2Q_0}{\omega_0} \quad \text{filling time constant} \quad (138)$$

If the cavity is equipped with a power coupler, we have to consider the ‘loaded Q ’ (which will be derived later), and the filling time constant changes to

$$\tau_1 = \frac{2Q_1}{\omega_0} \quad \text{filling time constant for a loaded cavity} \quad (139)$$

In the above definition, the electric field decays exponentially with a time constant $1/\tau$, whereas the

stored energy decays with a time constant $2/\tau$. Be aware that you can often find textbook definitions of the filling time constant where the stored energy decays with a time constant $1/\tau$.

4.6 Basic cavity parameters for a pillbox cavity

As a small exercise, in this section we calculate the cavity parameters that were defined in the previous section for a pillbox cavity of length L and radius a . Since the TM_{010} mode has no z dependence, we can simplify the expression for the transit time factor (127) to

$$T = \frac{\int_{-L/2}^{L/2} E(0, z) \cos(2\pi z/\beta\lambda) dz}{\int_{-L/2}^{L/2} E(0, z) dz} = \frac{\sin(\pi L/\beta\lambda)}{\pi L/\beta\lambda}. \quad \text{transit time factor of a pillbox for small velocity changes} \quad (140)$$

In the case of relativistic particles ($\beta \approx 1$) and a cavity length $L = \lambda/2$, which is often chosen because the cavity can then be cascaded into a multicell structure, we obtain

$$T = \frac{2}{\pi} = 0.64. \quad \text{transit time factor of a pillbox for relativistic particles} \quad (141)$$

With real cavities, one usually tries to increase the transit time factor by shortening the accelerating gap. This can be done by introducing nose cones on the cavity walls, as shown in Fig. 22.

We use the power loss method again to calculate the quality factor of our pillbox cavity. To evaluate Eq. (134), we need the stored energy and the power lost in the cavity walls. For the stored energy, we obtain

$$W = W_{\text{el}} + W_{\text{mag}} = 2W_{\text{el}} = 2 \int_V \frac{1}{4} \mathbf{E} \cdot \mathbf{D}^* dV. \quad (142)$$

With

$$E_z = E_0 J_0 \left(\frac{j_{01} r}{a} \right), \quad (143)$$

we obtain

$$W = \frac{\epsilon_0}{2} \int_0^a \int_0^{2\pi} \int_{-L/2}^{L/2} E_0^2 J_0^2 \left(\frac{j_{01} r}{a} \right) r dr d\phi dz = \frac{1}{2} E_0^2 \epsilon_0 \pi L a^2 J_1^2(j_{01}). \quad (144)$$

To calculate the dissipated power, we integrate Eq. (108) over a volume that consists of the inner surface of the pillbox times the skin depth:

$$P_d = \frac{\delta_s}{2\kappa} \int_{-L/2}^{L/2} \underbrace{J_z J_z^*}_{(1/\delta_s)^2 H_\phi^2(r=a, z)} 2\pi a dz + \frac{\delta_s}{\kappa} \int_0^a \underbrace{J_r J_r^*}_{(1/\delta_s)^2} H_\phi^2(r, z=0) 2\pi r dr \quad (145)$$

$$= \frac{E_0^2 \pi R_{\text{surf}} a}{Z_0^2} J_1^2(j_{01})(a+L), \quad (146)$$

where we have made use of

$$H_\phi = \frac{E_0}{Z_0} J_1 \left(\frac{j_{01} r}{a} \right). \quad (147)$$

Putting everything together, we obtain

$$Q_0 = \frac{\omega W}{P_d} = \frac{Z_0^2 \omega}{2R_{\text{surf}}} \frac{La}{L+a} = \frac{1}{\delta_s} \frac{La}{L+a} \propto \sqrt{\omega}. \quad (148)$$

As we can see, the quality factor is a function of the material constants κ and μ (which are contained in ρ_s), the frequency, and the geometry of the cavity. We also note that for the same cavity shape, the quality factor increases with the frequency in proportion to $\sqrt{\omega}$.

The accelerating voltage in a pillbox cavity is given by

$$V_{\text{acc}} = V_0 T = E_0 L T = E_0 L \frac{\sin(\pi L / \beta \lambda)}{\pi L / \beta \lambda}, \quad \text{accelerating voltage in pillbox} \quad (149)$$

and is obviously a strong function of the transit time factor. It therefore depends on the gap length L and the speed of the particles β . Owing to their high development costs, superconducting cavities are often used over large velocity ranges without changing their cell length, and this results in a velocity-dependent acceleration efficiency. Figure 26 shows $(R/Q) \propto (V_0 T)^2$ as a function of particle velocity for a five-cell superconducting cavity whose geometric cell length corresponds to a particle speed of $\beta = 0.65$.

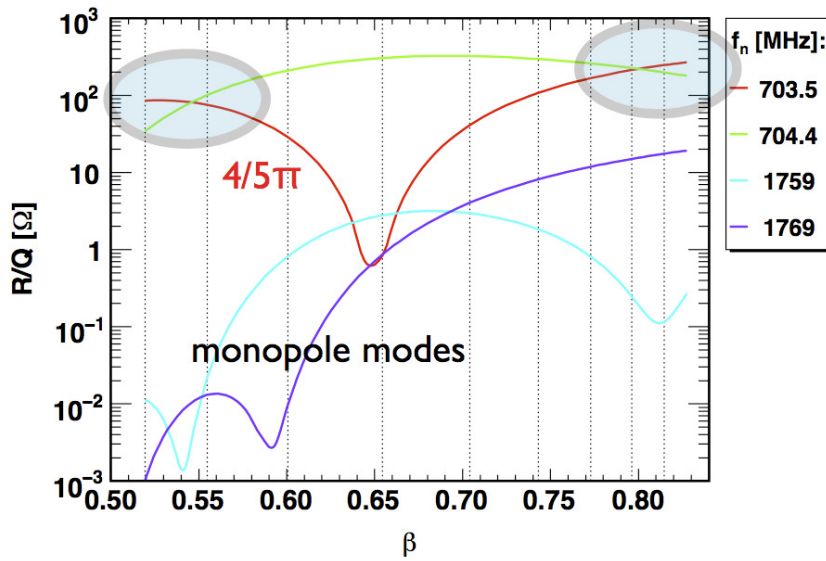


Fig. 26: Dependence of (R/Q) on particle velocity for a five-cell superconducting cavity with a geometric β of 0.65 and a frequency of 704.4 MHz. Upper curve, π mode (see also [15]).

If the cavity is used over too large a velocity range, one may find areas where the passband mode that is closest to the π mode (here, the $4/5\pi$ mode) has a higher acceleration efficiency than the accelerating mode. These areas are highlighted in Fig. 26, and should be avoided when one is designing a linac. One should also be aware that the (R/Q) of the HOMs is highly dependent on the particle velocity.

Using the expressions for the accelerating voltage $V_0 T$ (Eq. (149)) and the dissipated power P_d (Eq. (146)), we also obtain an analytical expression for the effective shunt impedance,

$$R = \frac{(V_0 T)^2}{P_d} = \frac{Z_0}{\pi R_{\text{surf}} J_1^2(j_{01})} \frac{\sin(\pi L / \beta \lambda)}{\pi L / \beta \lambda} \frac{L^2}{a(a+L)}. \quad \text{effective shunt impedance of a pillbox} \quad (150)$$

Finally, we calculate the frequency and (R/Q) using Eqs. (120), (150), and (148):

$$f_{010}^{\text{TM}} = \frac{2.405c}{2\pi a}, \quad \text{pillbox frequency} \quad (151)$$

$$\left(\frac{R}{Q}\right) = \frac{2c}{\omega\pi J_1^2(j_{01})} \frac{\sin(\pi L/\beta\lambda)}{\pi L/\beta\lambda} \frac{L}{a^2}. \quad \text{pillbox (R/Q)} \quad (152)$$

As stated before, (R/Q) is indeed independent of any material parameters. However, it does depend on the geometry of the cavity and the transit time factor.

4.7 A cavity as a lumped circuit

In the field of RF technology, it is common practice to describe the behaviour of cavities, RF transmission lines, and couplers with equivalent lumped circuits. In this chapter, we shall present only the treatment of a cavity and a coupler, so that one can understand how to get power into a cavity. Descriptions of the transmission of RF power and the associated theory of RF transmission lines can be found in many textbooks on RF and microwave engineering. We start with the description of a cavity by a parallel LCR circuit as depicted in Fig. 27.

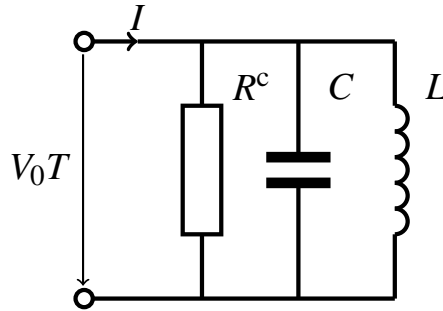


Fig. 27: Lumped-circuit equivalent of a resonant cavity

You may remember that the admittance of a parallel circuit is calculated by adding up the admittances of the individual elements, which means that we can write the cavity impedance as

$$Z^c = \frac{1}{i\omega C + 1/i\omega L + 1/R^c}. \quad \text{lumped-circuit cavity impedance} \quad (153)$$

At resonance ($\omega = \omega_0$), the imaginary parts cancel each other and the cavity impedance becomes real, which means that

$$X = \omega_0 L = \frac{1}{\omega_0 C} = \sqrt{\frac{L}{C}}, \quad \text{lumped circuit at resonance} \quad (154)$$

that the resonance frequency is given by

$$\omega_0 = \frac{1}{\sqrt{LC}}, \quad \text{lumped-circuit resonance frequency} \quad (155)$$

and that the power lost in the resonator is given by

$$P_d = \frac{1}{2} \frac{(V_0 T)^2}{R^c}. \quad \text{lumped-circuit dissipated power} \quad (156)$$

The stored energy can be written as

$$W = \frac{1}{2}C(V_0T)^2 = \frac{1}{2}\frac{(V_0T)^2}{\omega_0^2L}, \quad \text{lumped-circuit stored energy} \quad (157)$$

and from this we obtain an expression for the quality factor,

$$Q_0 = \omega_0 \frac{W}{P_d} = \omega_0 CR^c = \frac{R^c}{\omega_0 L}. \quad \text{lumped-circuit quality factor} \quad (158)$$

Our goal is to relate the lumped elements to the cavity characteristics, and for this purpose we multiply Eq. (157) by ω and, together with Eq. (154), we obtain

$$\frac{1}{\omega_0 C} = \sqrt{\frac{L}{C}} = \frac{(V_0T)^2}{2\omega_0 W} = \left(\frac{R^c}{Q}\right) = \frac{1}{2}\left(\frac{R}{Q}\right). \quad (159)$$

From this, we can understand the difference between the ‘circuit ohm’ and the ‘linac ohm’, and it also provides a lumped-circuit description of a cavity, as summarized in Table 1. As we can see, three quantities are sufficient to describe a resonator. Instead of using R , L , and C , one can also use the parameters ω_0 , Q_0 , and (R/Q) to completely characterize an RF cavity, as in Table 2.

Table 1: Lumped-circuit elements of a cavity

Lumped circuit	Field description
R^c	$\frac{1}{2}R$
C	$\frac{2}{\omega_0(R/Q)}$
L	$\frac{1}{2\omega_0}\left(\frac{R}{Q}\right)$

Table 2: Three characteristic quantities of a cavity

Lumped circuit	Field description
$\omega_0 = \frac{1}{\sqrt{LC}}$	$\frac{2.405c}{a}$ (pillbox)
$Q_0 = \omega_0 CR^c = \frac{R^c}{\omega_0 L}$	$Q_0 = \frac{\omega_0 W}{P_d}$
$\left(\frac{R^c}{Q}\right) = \sqrt{\frac{L}{C}} = \frac{1}{2}\left(\frac{R}{Q}\right)$	$\left(\frac{R}{Q}\right) = \frac{(V_0T)^2}{\omega_0 W}$

4.8 Getting power into a cavity: couplers

In this section, we shall extend the circuit model to include the power coupler and also extend our basic equations to describe the process of coupling power into a cavity. There are two basic types of couplers

that are used in standing-wave cavities:

- *Antenna/loop couplers*: here, the coupler is usually some kind of coaxial line, with the outer conductor connected to the cavity wall and the inner conductor either penetrating into the cavity volume or connected in a loop to the inner surface of the cavity (Fig. 28).
- *Iris couplers*: here, the fields in a waveguide are coupled to the cavity fields via an opening that connects the waveguide to the cavity.

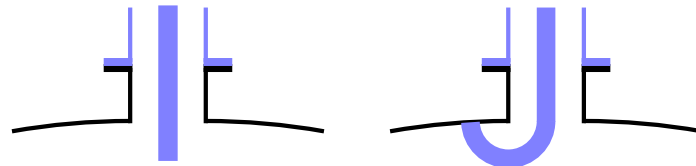


Fig. 28: Example of an antenna-type coupler (left) and a loop-type coupler (right)

When designing a coupler, one has to keep in mind the principle of reciprocity: the coupler has to produce a field pattern in the area of the coupling port that is very similar to the field pattern of the mode that will be excited in the cavity. Looking at Fig. 28, one can imagine that an antenna-type coupler would be very effective on the end walls of our pillbox, where it would couple electrically to the axial electric field lines. On the cylindrical surface of the pillbox, a loop coupler would be a better choice, with the loop oriented such that the azimuthal magnetic field penetrates the loop.

Figure 29 shows an example of a ‘tuner-adjustable (waveguide) coupler’ (TaCo) [16], as used for the Linac4 [17] cavities at CERN. In this case a short-circuited rectangular waveguide is coupled to a standing-wave cavity via a racetrack-shaped coupling iris. The coupling factor (more on this later) here is a function of the position of the short circuit (left side), the height of the racetrack-shaped coupling channel between the cavity and the waveguide (on the top), the size of the coupling slot, and the position of a stub tuner, which is used to fine-tune the coupling.

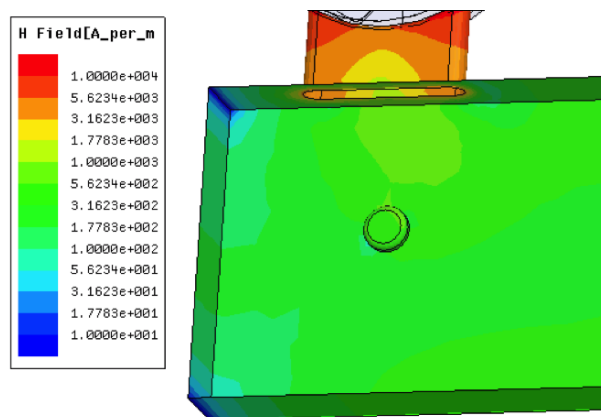


Fig. 29: Waveguide coupler connected to a Linac4 cavity

In the ideal case, the power coupler is matched to the (beam-)loaded cavity, which means that there is no reflected power returning from the cavity towards the RF power source. Here, ‘matched’ means that the coupler acts like an ideal transformer that transforms the impedance Z_c of the cavity into the impedance Z_0 of the attached waveguide. To keep things simple, let us assume that the RF generator is also matched to Z_0 so that we can establish a lumped-element circuit as shown in Fig. 30.

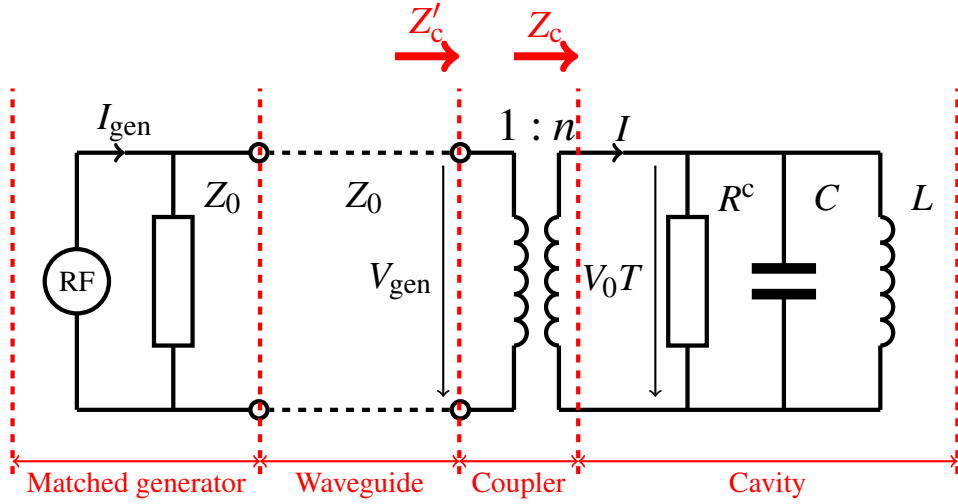


Fig. 30: Lumped-element circuit for RF power source, waveguide, power coupler, and cavity

Considering the coupler as a transformer, we can write that

$$\left. \begin{aligned} V_0 T &= n V_{\text{gen}} \\ I &= \frac{I_{\text{gen}}}{n} \end{aligned} \right\} \Rightarrow Z_c = \frac{V_0 T}{I} = n^2 Z'_c, \quad (160)$$

which means that the cavity impedance

$$Z_c = \frac{1}{i\omega C + 1/i\omega L + 1/R^c} \quad \text{cavity impedance} \quad (161)$$

is transformed into

$$Z'_c = \frac{1}{i\omega n^2 C + n^2/i\omega L + n^2/R^c}, \quad \text{cavity + coupler impedance} \quad (162)$$

which is the impedance ‘seen’ from the waveguide. The stored energy in the resonator, expressed in lumped-circuit values, becomes

$$W = \frac{C}{2(V_0 T)^2} = n^2 \frac{C}{2V_{\text{gen}}^2}, \quad \text{stored energy} \quad (163)$$

and the dissipated power can be written as

$$P_d = \frac{(V_0 T)^2}{2R^c} = n^2 \frac{V_{\text{gen}}^2}{2R^c}. \quad \text{dissipated power} \quad (164)$$

Now we can define the quality factor of the unloaded cavity with lumped-circuit elements:

$$Q_0 = \frac{\omega_0 W}{P_d} = \omega_0 R^c C. \quad \text{unloaded } Q \quad (165)$$

When the generator is switched off, not only will the stored energy in the cavity be dissipated in the cavity walls, but a power P_{ex} will also leak out through the power coupler, where

$$P_{\text{ex}} = \frac{V_{\text{gen}}^2}{2Z_0}. \quad (166)$$

Using P_{ex} , one can define the quality factor of the external load. The external Q is thus defined as

$$Q_{\text{ex}} = \frac{\omega_0 W}{P_{\text{ex}}} = n^2 \omega_0 Z_0 C. \quad \text{external } Q \quad (167)$$

4.8.1 Undriven cavity

In order to understand the power balance and matching for a driven cavity with beam, we start with a simple case, assuming that the RF is switched off and that there is no beam in the cavity. The power balance is then

$$P_{\text{tot}} = P_{\text{d}} + P_{\text{ex}}, \quad \text{power balance of undriven cavity} \quad (168)$$

with which we can define the so-called ‘loaded Q ’ of the ensemble of cavity and coupler by

$$\frac{1}{Q_{\text{l}}} = \frac{1}{Q_{\text{ex}}} + \frac{1}{Q_0}. \quad \text{loaded } Q \quad (169)$$

The coupling between the cavity and the waveguide is described by the coupling factor β , where

$$\beta = \frac{P_{\text{ex}}}{P_{\text{d}}} = \frac{Q_0}{Q_{\text{ex}}} = \frac{R^{\text{c}}}{n^2 Z_0}. \quad \text{coupling factor} \quad (170)$$

Optimum power transfer between the cavity (+ coupler) and the waveguide takes place when the impedance at the coupler input equals the waveguide impedance at the resonance frequency of the cavity. We know that the cavity impedance becomes real at resonance, which means that

$$Z_{\text{c}} = R^{\text{c}} = n^2 Z_{\text{c}}' \stackrel{!}{=} n^2 Z_0 \quad \Rightarrow \quad \beta = 1. \quad (171)$$

It is important to keep in mind that the ‘matching condition’ $\beta = 1$ is only valid for a cavity without beam.

4.8.2 RF on, beam on

Once we take the beam loading into account, the power needed in the cavity increases and will yield a different value for the coupling factor β at the point of optimum power transfer. A simple way to introduce the beam is to treat it as an additional loss in the cavity, which can be added to the power dissipated in the cavity walls:

$$P_{\text{db}} = P_{\text{d}} + P_{\text{b}}. \quad \text{dissipated power + beam power} \quad (172)$$

As in the case without beam, maximum power transfer to the cavity is achieved when the input impedance of the coupler equals the impedance of the waveguide. This condition yields zero reflection and also implies that the power needed in the cavity, P_{db} (for losses and beam), has to be equal to P_{ex} as defined in Eq. (166). This means that

$$\frac{P_{\text{ex}}}{P_{\text{db}}} = 1 = \frac{Q_{0\text{b}}}{Q_{\text{ex}}} \quad \Rightarrow \quad \frac{P_{\text{ex}}}{P_{\text{d}}} = 1 + \frac{P_{\text{b}}}{P_{\text{d}}}, \quad (173)$$

where we have introduced a quality factor Q_{0b} for the cavity plus beam. For the matched condition, we therefore obtain a coupling factor of

$$\beta = 1 + \frac{P_b}{P_d}, \quad \text{matched coupling factor with beam} \quad (174)$$

and the following quality factors:

$$Q_{\text{ex}} = Q_{0b} = \frac{\omega_0 W}{P_b + P_d} = \frac{Q_0}{1 + P_b/P_d} = \frac{Q_0}{\beta}, \quad \text{external } Q \text{ with beam} \quad (175)$$

$$Q_1 = \frac{Q_0}{1 + \beta} = \frac{Q_0}{2 + P_b/P_d}. \quad \text{loaded } Q \text{ with beam} \quad (176)$$

In the case of a superconducting cavity, one can generally assume that $P_b \gg P_d$, which means that the coupling factor for the matched condition can be written as

$$\beta = 1 + \frac{P_b}{P_d} \approx \frac{P_b}{P_d}. \quad \text{matched coupling factor for SC cavity + beam} \quad (177)$$

Using

$$P_b = I_{\text{beam}} V_0 T \cos \phi_s, \quad (178)$$

we can write a simple expression for calculating the loaded and external Q values for a superconducting cavity as follows:

$$Q_1 \approx Q_{\text{ex}} \approx \frac{Q_0}{P_{\text{beam}}/P_d} = \frac{V_0 T}{(R/Q) I_{\text{beam}} \cos \phi_s}. \quad Q_{1/\text{ex}} \text{ for SC cavity} \quad (179)$$

The results in this paragraph are summarized in Table 3.

Table 3: Definitions of Q values and coupling factors for driven and undriven cavities

	Undriven cavity	Driven cavity
General	$\frac{1}{Q_1} = \frac{1}{Q_{\text{ex}}} + \frac{1}{Q_0}$ $\beta = \frac{P_{\text{ex}}}{P_d} = \frac{Q_0}{Q_{\text{ex}}}$ $Q_1 = \frac{Q_0}{1 + \beta}$	
Matched case	$\frac{P_{\text{ex}}}{P_d} = \frac{Q_0}{Q_{\text{ex}}} = 1 \Rightarrow \beta = 1$ $Q_{\text{ex}} = Q_0 = \frac{\omega_0 W}{P_d}$ $Q_1 = \frac{Q_0}{2}$	$\frac{P_{\text{ex}}}{P_{\text{db}}} = \frac{Q_{0b}}{Q_{\text{ex}}} = 1 \Rightarrow \beta = 1 + \frac{P_b}{P_d}$ $Q_{\text{ex}} = Q_{0b} = \frac{\omega_0 W}{P_d + P_b}$ $Q_1 = \frac{Q_0}{2 + P_b/P_d}$

4.9 ‘Matching’ a cavity

In the last section, it was claimed that part of an electromagnetic wave is reflected when it ‘sees’ a change in impedance during its propagation. In fact, the whole purpose of the power coupler was to transform the impedance of the waveguide into the impedance of the cavity. In this last section, we shall see why this is so. For this purpose, we look at a transmission line as shown in Fig. 31.

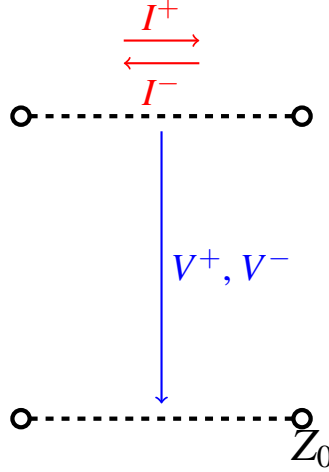


Fig. 31: Voltages and currents along a transmission line

This transmission line is representative of a waveguide, a coaxial line, or any other kind of transport geometry used to guide electromagnetic waves. Since waves can travel in the positive and negative z directions, a sign convention is introduced for the associated voltages and currents, as shown in Fig. 31, where the voltage vectors of the forward and reflected waves have the same direction and the current vectors have opposite directions.

Using the same time and location dependence as for the electric and magnetic fields in a waveguide, we can write

$$V = V_0 e^{i(kz - \omega t)} + \Gamma V_0 e^{i(-kz - \omega t)}, \quad (180)$$

$$I = \frac{V_0}{Z_0} e^{i(kz - \omega t)} - \Gamma \frac{V_0}{Z_0} e^{i(-kz - \omega t)}, \quad (181)$$

where we have introduced a reflection coefficient Γ . If we connect a cavity to an impedance Z'_c at $z = 0$, the expressions above simplify to

$$V = V_0 e^{-i\omega t} (1 + \Gamma), \quad (182)$$

$$I = \frac{V_0}{Z_0} e^{-i\omega t} (1 - \Gamma), \quad (183)$$

and the cavity impedance can be expressed in terms of the transmission line impedance Z_0 and the reflection coefficient Γ :

$$Z'_c = \frac{V}{I} = Z_0 \frac{1 + \Gamma}{1 - \Gamma}. \quad (184)$$

We can then rearrange the equation for the reflection coefficient and obtain

$$\Gamma = \frac{Z'_c - Z_0}{Z'_c + Z_0} = \frac{1 - \beta}{1 + \beta}. \quad (185)$$

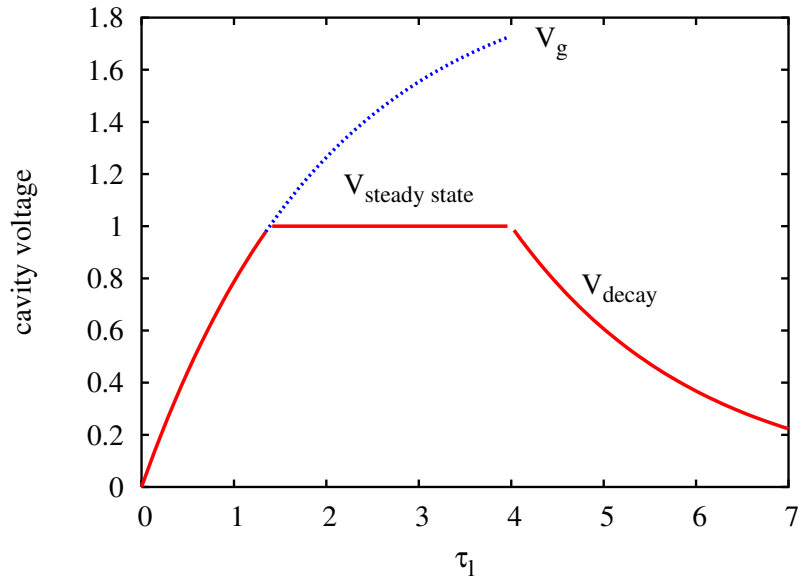


Fig. 32: Voltage profile in a pulsed superconducting cavity

From this equation, we can see that the reflection disappears only for $Z'_c = Z_0$, the ‘matched condition’, where the waveguide impedance equals the cavity impedance. In the case without beam, this corresponds to a coupling factor of $\beta = 1$.

In the context of matching, we therefore have to consider the following points:

- At the resonance frequency, the power coupler transforms the cavity impedance into the impedance of the waveguide.
- If the cavity is resonating off-resonance or if the coupler is mismatched, power is reflected and travels back to the RF source.
- Since the cavity impedance depends on the Q of the cavity, and since in reality most cavities have different Q values, every cavity needs a different matching.
- Beam loading increases the power needed in the cavity and changes the loaded Q and the cavity impedance. Power couplers are usually matched for the case with beam loading.
- During the start of an RF pulse (before the arrival of the beam), when the cavity is being ‘filled’ with RF power, the cavity is always mismatched, which means we need to make sure that the reflected power does not damage the RF source (e.g., by using a circulator between the cavity and the RF source).

The last point is especially important in the case of superconducting cavities, where the dissipated power is negligible with respect to the power taken by the beam. In this case one has, basically, full reflection of the RF wave at the beginning of the RF pulse before the cavity field increases to its nominal level. At that point the beam should enter the cavity, and from then onwards the RF generator is matched to the power needs of the RF cavity. After the RF signal is switched off, the cavity voltage decays exponentially, as shown in Fig. 32 (more details can be found in [18]).

Acknowledgements

In the preparation of this chapter, I have made extensive use of the material listed in the Bibliography below.

References

- [1] R.P. Feynman, R.B. Leighton, and M. Sands, *The Feynman Lectures on Physics*, Vol. II, *Mainly Electromagnetism and Matter* (California Institute of Technology, 1963).
- [2] H. Henke, *Theoretische Elektrotechnik*, German script of lectures on electrodynamics at the Technical University of Berlin (1992).
- [3] T. Weiland, M. Krasilnikov, R. Schuhmann, A. Skarlatos, and M. Wilke, Review of theory (I, II, III), CAS RF Engineering, Seeheim, Germany (2005).
- [4] M. Abramowitz and I.A. Stegun, *Handbook of Mathematical Functions* (Dover Publications, New York, 1965).
- [5] T. Wangler, *Principles of RF Linear Accelerators* (Wiley-VCH, Weinheim, 2004).
- [6] M. Vretenar, Low-beta structures, CAS RF School, Ebeltoft, Denmark (2010).
- [7] D.E. Nagle, E.A. Knapp, and B.C. Knapp, *Rev. Sci. Instrum.* **38** (1967) 1583.
- [8] S. Schriber, Characteristics of full-cell terminated RF structures: results of analogue studies, CERN/PS/2001-067 (PP) (2001).
- [9] S. Schriber, *Phys. Rev. ST Accel. Beams* **4** (2001) 122001.
- [10] The Compact Linear Collider Study, <http://www.cern.ch/clic-study>.
- [11] International Linear Collider, <http://www.linearcollider.org>.
- [12] R.H. Miller, Comparison of standing wave and travelling wave structures, LINAC86 (1986).
- [13] V.A. Moiseev, V.V. Paramonov, and K. Floettmann, Comparison of standing and travelling wave operations for positron pre-accelerator in the TESLA Linear Collider, EPAC (2000).
- [14] F. Gerigk, Cavity types, CAS RF School, Ebeltoft, Denmark, arXiv:1111.4897v1 (2010).
- [15] M. Schuh, F. Gerigk, J. Tuckmantel, and C.P. Welsch, Influence of higher order modes on the beam stability in the high power superconducting proton linac, *Phys. Rev. ST Accel. Beams* **14** (2011) 051001.
- [16] F. Gerigk, J.M. Giguët, E. Montesinos, B. Riffaud, P. Ugena Tirado, and R. Wegner, The Linac4 power coupler, IPAC 2011, San Sebastian, Spain, CERN-ATS-2011-040 (2011).
- [17] M. Vretenar *et al.*, The LINAC4 project at CERN, IPAC 2011, San Sebastian, Spain, CERN-ATS-2011-041 (2011).
- [18] F. Gerigk, Formulae to calculate the power consumption of the SPL SC cavities, CERN-AB-Note-2006-011-RF (2006).

Bibliography

- T. Weiland, M. Krasilnikov, R. Schuhmann, A. Skarlatos, and M. Wilke, Review of theory (I, II, III), CAS RF Engineering, Seeheim, Germany (2005).
- T. Wangler, *Principles of RF Linear Accelerators* (Wiley-VCH, Weinheim, 2004).
- A. Wolski, Theory of electromagnetic fields, CAS RF Engineering, Ebeltoft, Denmark (2010).
- H. Henke, *Theoretische Elektrotechnik*, German script of lectures on electrodynamics at the Technical University of Berlin (1992)
- H. Henke, Basic concepts I and II, CAS RF Engineering, Seeheim, Germany (2005).
- K. Simonyi, *Foundations of Electrical Engineering*, Vol. 3 (Pergamon Press, New York, 1963). [Hungarian edition, *Elm lleti villamossagtan Tankonyvkiado* (Budapest, 1973); German edition, *Theoretische Elektrotechnik* (VEB Deutscher Verlag der Wissenschaften, 1973).]
- H. Padamsee, J. Knobloch, and T. Hays, *RF Superconductivity for Accelerators* (Wiley, New York, 2008).

Appendices

A Cartesian coordinates (x, y, z)

A.1 Differential elements

$$d\mathbf{l} = \begin{pmatrix} dx \\ dy \\ dz \end{pmatrix}, \quad \text{path element} \quad (\text{A.1})$$

$$dV = dx dy dz. \quad \text{volume element} \quad (\text{A.2})$$

A.2 Differential operators

$$\nabla\phi = \begin{pmatrix} \frac{\partial\phi}{\partial x} \\ \frac{\partial\phi}{\partial y} \\ \frac{\partial\phi}{\partial z} \end{pmatrix}, \quad \text{gradient} \quad (\text{A.3})$$

$$\nabla \cdot \mathbf{a} = \frac{\partial a_x}{\partial x} + \frac{\partial a_y}{\partial y} + \frac{\partial a_z}{\partial z}, \quad \text{divergence} \quad (\text{A.4})$$

$$\nabla \times \mathbf{a} = \begin{pmatrix} \frac{\partial a_z}{\partial y} - \frac{\partial a_y}{\partial z} \\ \frac{\partial a_x}{\partial z} - \frac{\partial a_z}{\partial x} \\ \frac{\partial a_y}{\partial x} - \frac{\partial a_x}{\partial y} \end{pmatrix}, \quad \text{curl} \quad (\text{A.5})$$

$$\Delta\phi = \frac{\partial^2\phi}{\partial x^2} + \frac{\partial^2\phi}{\partial y^2} + \frac{\partial^2\phi}{\partial z^2}. \quad \text{Laplace} \quad (\text{A.6})$$

B Cylindrical coordinates (r, ϕ, z)

B.1 Transformations

$$\begin{aligned} x &= r \cos \phi, \\ y &= r \sin \phi, \\ z &= z, \end{aligned} \quad (\text{B.1})$$

with $0 \leq r \leq \infty, 0 \leq \phi \leq 2\pi$.

B.2 Differential elements

$$d\mathbf{l} = \begin{pmatrix} dr \\ r d\varphi \\ dz \end{pmatrix}, \quad \text{path element} \quad (\text{B.2})$$

$$dV = r dr d\varphi dz. \quad \text{volume element} \quad (\text{B.3})$$

B.3 Differential operators

$$\nabla\phi = \begin{pmatrix} \frac{\partial\phi}{\partial r} \\ \frac{1}{r} \frac{\partial\phi}{\partial\varphi} \\ \frac{\partial\phi}{\partial z} \end{pmatrix}, \quad \text{gradient} \quad (\text{B.4})$$

$$\nabla \cdot \mathbf{a} = \frac{1}{r} \frac{\partial(ra_r)}{\partial r} + \frac{1}{r} \frac{\partial a_\varphi}{\partial\varphi} + \frac{\partial a_z}{\partial z}, \quad \text{divergence} \quad (\text{B.5})$$

$$\nabla \times \mathbf{a} = \begin{pmatrix} \frac{1}{r} \frac{\partial a_z}{\partial\varphi} - \frac{\partial a_\varphi}{\partial z} \\ \frac{\partial a_r}{\partial z} - \frac{\partial a_z}{\partial r} \\ \frac{1}{r} \left(\frac{\partial(ra_\varphi)}{\partial r} - \frac{\partial a_r}{\partial\varphi} \right) \end{pmatrix}, \quad \text{curl} \quad (\text{B.6})$$

$$\Delta\phi = \frac{\partial^2\phi}{\partial r^2} + \frac{1}{r} \frac{\partial\phi}{\partial r} + \frac{1}{r^2} \frac{\partial^2\phi}{\partial\varphi^2} + \frac{\partial^2\phi}{\partial z^2}. \quad \text{Laplace} \quad (\text{B.7})$$

C Spherical coordinates (r, ϑ, φ)

C.1 Transformations

$$\begin{aligned} x &= r \sin \vartheta \cos \varphi, \\ y &= r \sin \vartheta \sin \varphi, \\ z &= r \cos \vartheta, \end{aligned} \quad (\text{C.1})$$

with $0 \leq r \leq \infty$, $0 \leq \vartheta \leq \pi$, $0 \leq \varphi \leq 2\pi$.

C.2 Differential elements

$$d\mathbf{l} = \begin{pmatrix} dr \\ r d\vartheta \\ r \sin \vartheta d\varphi \end{pmatrix}, \quad \text{path element} \quad (\text{C.2})$$

$$dV = r^2 \sin \vartheta dr d\vartheta d\varphi. \quad \text{volume element} \quad (\text{C.3})$$

C.3 Differential operators

$$\nabla\phi = \begin{pmatrix} \frac{\partial\phi}{\partial r} \\ \frac{1}{r} \frac{\partial\phi}{\partial\vartheta} \\ \frac{1}{r \sin \vartheta} \frac{\partial\phi}{\partial\varphi} \end{pmatrix}, \quad \text{gradient} \quad (\text{C.4})$$

$$\nabla \cdot \mathbf{a} = \frac{1}{r^2} \frac{\partial(r^2 a_r)}{\partial r} + \frac{1}{r \sin \vartheta} \frac{\partial(a_\vartheta \sin \vartheta)}{\partial \vartheta} + \frac{1}{r \sin \vartheta} \frac{\partial a_\varphi}{\partial \varphi}, \quad \text{divergence} \quad (\text{C.5})$$

$$\nabla \times \mathbf{a} = \begin{pmatrix} \frac{1}{r \sin \vartheta} \left(\frac{\partial(a_\varphi \sin \vartheta)}{\partial \vartheta} - \frac{\partial a_\vartheta}{\partial \varphi} \right) \\ \frac{1}{r} \left(\frac{1}{\sin \vartheta} \frac{\partial a_r}{\partial \varphi} - \frac{\partial(r a_\varphi)}{\partial r} \right) \\ \frac{1}{r} \left(\frac{\partial(r a_\vartheta)}{\partial r} - \frac{\partial a_r}{\partial \vartheta} \right) \end{pmatrix}, \quad \text{curl} \quad (\text{C.6})$$

$$\Delta\phi = \frac{\partial^2\phi}{\partial r^2} + \frac{2}{r} \frac{\partial\phi}{\partial r} + \frac{1}{r^2 \sin \vartheta} \frac{\partial}{\partial \vartheta} \left(\sin \vartheta \frac{\partial\phi}{\partial \vartheta} \right) + \frac{1}{r^2 \sin^2 \vartheta} \frac{\partial^2\phi}{\partial \varphi^2}. \quad \text{Laplace} \quad (\text{C.7})$$

D Useful relationships

$$\nabla \cdot (\mathbf{a} \times \mathbf{b}) = \mathbf{b} \cdot (\nabla \times \mathbf{a}) - \mathbf{a} \cdot (\nabla \times \mathbf{b}), \quad (\text{D.1})$$

$$\nabla \cdot (\nabla \times \mathbf{a}) = 0. \quad (\text{D.2})$$